

Spectrum



Winter 2022 | Issue 104

'CONDITION MONITORING IN A CHANGING WORLD'

Conference 2022 is here!

Taupo - 16th, 17th and 18th August



Effect of Vibration and
Noise Measuring Points
Distribution on the

Sensitivity of Pump Cavitation Diagnosis

Skills & Practices

Soft Foot on Belt
Drive Motors...



**15%
DISCOUNT
AVAILABLE!**

Read on to find out if you're eligible!

VANZ

VIBRATIONS ASSOCIATION of NEW ZEALAND



PRESENTS...

CONFERENCE '22

'CONDITION MONITORING IN A CHANGING WORLD'

Wairakei Resort, Taupo

16th, 17th and 18th August 2022

Tuesday 16th offers **FREE** attendance for apprentices!

Registration has never been easier!

Registration for the 2022 VANZ Conference is easy. Simply click on or visit www.vanz.org.nz and fill in the details online, or scan* the QR code below, and it will take you directly to the online registration form.



* QR Code scanner app required for mobile device to enable scanning. Available from all app stores.



Did you know you might be eligible to receive 15% off!

If you registered for the 2021 Conference last year, you will be receiving a unique code sent to your business address. Grab the code, visit www.vanz.org.nz/conference-2022, register for the 2022 Conference and enter your unique code when prompted.

Success!



John van Zwienen



Dr Iain Epps



Dare Petreski



Mike Davis

CONFERENCE '22 SPEAKER BIOS

Here is a little background on some of the key presenters you'll hear at the upcoming VANZ Conference in Taupo.

1. John van Zwienen

Sales Manager with 40+ years hands-on experience in all aspects of Rotating Machinery Vibration business. Category IV Vibration Analyst. Skilled in Gas Turbine & Steam Turbine driven Power Plants, Refineries, and General Manager Sales & Service at BK Vibro.

2. Dr Iain Epps

Recognised around the world for his research into the origins of machine vibrations and the holder of several patents on condition monitoring.

3. Dare Petreski

Asset Management, Maintenance & Reliability Improvement Professional [CMRP] An accomplished speaker and training facilitator. Twenty-five years of progressive experience in Physical Asset Management, and Risk Mitigation and more.

4. Mike Davis

An Electrical Engineer, "I coach users of electrical machinery to understand failure processes and run equipment at optimum levels to prevent costly break downs."



We'll see you there...

Share knowledge, passion and successes. Network and totally immerse yourself in this 3-day event!

Principal sponsor:

CSEW Arthur Fisher
a division of CSE New Zealand



Brüel & Kjær Vibro



Spectrum

INSIDE THIS ISSUE >

Features

Conference 2022 incl. full timetable

Skills and Practices

Soft foot on Belt Drive Motors

Vibration based condition monitoring of rotating part using spectrum analysis:
A case study on milling machine

Effect of vibration and noise measuring points distribution on the sensitivity of Pump Cavitation Diagnosis

Regulars

6	From the president	5
	Editor's report	12
	Test your knowledge	37
14	Puzzle corner	38

16

Missed an issue?

Simply scan the QR code here to link your device directly to the VANZ website. There you will find Spectrum issues available to view or download*.

*QR code reading app need on your device first.



20



Issue 104

Web Site: www.vanz.org.nz

Spectrum is published quarterly in a digital medium and printed twice yearly by the Vibration Association of New Zealand (VANZ). The magazine is designed to cover all aspects of the Vibration, Condition Monitoring, Reliability and the wider Predictive Asset Management field and distributed to all VANZ members, including corporate members.

Contributions to Spectrum are welcome.

Please address material to:
Angie Hurricks
Spectrum Editor
c/o 358 Waerenga Road,
R.D.1, Te Kauwhata, 3781
Waikato, New Zealand
or email: spectrumeditor@vanz.org.nz

Address all VANZ correspondence to:
VANZ
PO Box 2122,
Shortland Street
Auckland

Editor: Angie Hurricks
Ph 021 239 4572
Email: spectrumeditor@vanz.org.nz

President: Rodney Bell
Email: rodney@mbs.net.nz

Treasurer: Graeme Finch
Email: G.Finch@auckland.ac.nz

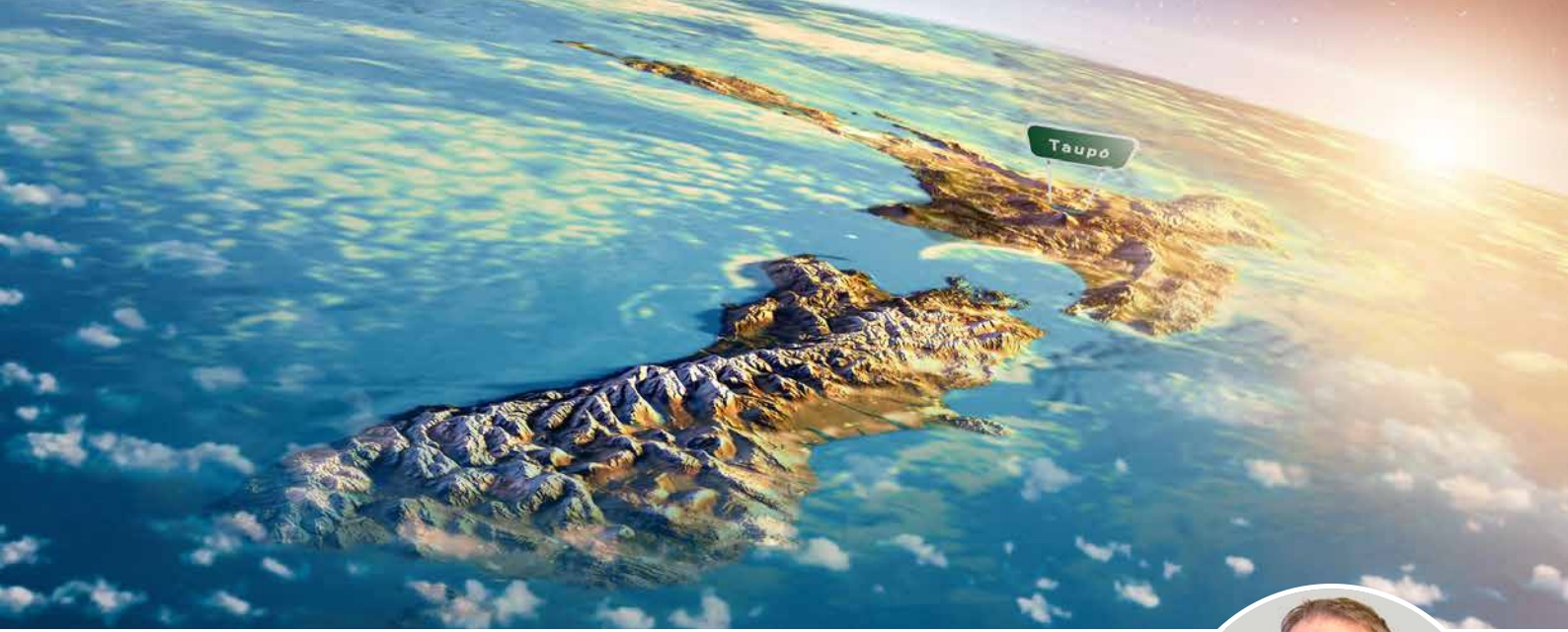
Secretary: Bill Sinclair
Email: bill.sinclair@valas.co.nz

Design: Eddie van den Broek
Flashpoint Design and Marketing
info@flashpoint.design

Statements made or opinions expressed in Spectrum are not necessarily the views of VANZ or its Officers and Committee.



ISSN 1173-793X



PRESIDENTS' REPORT

By Rodney Bell, VANZ President



Greetings to you all once again, the VANZ committee has been working hard and we are all now getting excited with the planning progress and looking forward to the execution of the annual VANZ Reliability Conference being held at the Wairakei Resort Taupo on August 16th 17th & 18th themed "Condition Monitoring In A Changing World".

We have confirmed Key-Note speaker John Van Zwiene who is General Manager Sales and Service (Asian & Oceania) for CSE-W Arthur Fisher. John has 40+ years hands-on experience in all aspects of Rotating Machinery Vibration business, a Category IV Vibration Analyst, skilled in Gas Turbine & Steam Turbine driven machines for Power Generation, Oil & Gas and Petrochemical Industries.

The Guest speaker lineup is also looking great with Dr Iain Epps, Daré Petreski and Mike Davis, all of whom have presented at VANZ on multiple occasions with excellent feedback from attendees. Bios for all are available at www.vanz.org.nz/conference-2022

Day 1 on the 16th is a split stream with the Asset Management/Reliability Day and the Practical Hands-on Awareness Day, the latter being free to all apprentices. In 2021 this day was a huge success, until Covid-19 put us all into lockdown again. This year is planned to be bigger & better, so I encourage all that are considering registering for VANZ 2022 to include this day in their package.

Day 2 & Day 3 are already packed full with split streams running, other than when there is live streaming or Key-Note presentations. A full mixture of presentations, covering Vibration, Laser Shaft Alignment, Ultra Sonics, Thermal Imaging, Safety & Reliability, Plant Reliability in general, Wireless Monitoring and a paper presented by Chris Pullen from Westland Milk Products about their sitewide journey to equipment reliability over an approx. 8-year period.

I look forward to welcoming all exhibitors and attendees to Wairakei Resort and spending time encouraging great learning throughout this event.

VANZ is an engineering technical platform for New Zealand and Australian engineering industry engaged in the technical disciplines of Predictive Asset Management, if your company is looking to begin or progress your plant's reliability program, I strongly encourage all to consider attending this year's annual conference.

Importantly during the networking events the exhibitors have their Condition Monitoring equipment on display ready to give demonstrations and to answer any questions. I personally believe 100% that for equipment reliability, this is the place to be and it's not too late to register.

I look forward to welcoming all exhibitors and attendees to the Wairakei Resort on the 16th 17th & 18th August 2022 and spending time encouraging great learning throughout this event. ■

CONFERENCE '22

Wairakei Resort, Taupo: 16th – 18th August

Australasia's Premier Annual 3-Day Predictive Asset Management and Reliability Condition Monitoring Event.

'CONDITION MONITORING IN A CHANGING WORLD'

SPECIAL OFFER!

DID YOU REGISTER FOR THE CONFERENCE LAST YEAR?

You and your business may be eligible for a **15% discount on 2022 prices.** Enter your unique code at www.vanz.org.nz to take advantage of this special offer!

TIMETABLE

Book online: www.vanz.org.nz

Tuesday, August 16th

Wednesday, August 17th

Thursday, August 18th

**3
DAY**

**Technology
Exhibition**

Visit 20+ world-leading condition monitoring and reliability providers showcasing their latest technologies all under one roof over all-three days of the conference.

**3
DAY**

Three-Day VANZ Conference Pass (Early Bird Pass*)

Get the full conference experience... See next page for full package pricing and details.

**1
DAY
OPT. 1**

**Practical
Hands-on
Awareness**

See next page for full package pricing and details.

**2
DAY**

Two-Day VANZ Conference Pass

See next page for full package pricing and details.

+ Networking and
Main Conference Dinner

+ Networking and
Social Event

**1
DAY
OPT. 2**

**Reliability/
Asset
Management**

See next page for full package pricing and details.

+ Networking and
Informal Welcome Evening

Membership up to date?

Full year for 2022/23 is only **\$100/pp**

It's easy to renew! Visit www.vanz.org.nz

If you purchase a Main Conference attendee pass, your membership for the next 12 months is automatically included and updated in that price.

pp = per person. * Early bird pass available until July 31st, 2022.

ACCOMMODATION

Use VANZ booking discount code: **vanz2022**

For the conference, we've secured rooms at Wairakei Resort, Taupo for a great rate if you need to book accommodation separately, but it's only for a limited time and availability will reduce closer to the conference date.

To reserve your room(s), phone Wairakei Resort on 07-374 8021, visit www.wairakei.co.nz or scan the QR code to link directly to their booking site.



ROOM RATES

First in first served!

**Special rates for VANZ
conference attendees!**

\$POA



CONFERENCE EVENING EVENTS

We will be hosting two evening events

Tuesday, 16th August

Informal Welcome Evening

Book online: www.vanz.org.nz for additional tickets.

Please advise attendance numbers for catering.

Additional tickets: \$25/pp

Wednesday, 17th August

Main Conference Dinner Event

Book online: www.vanz.org.nz for additional tickets.

This is a special event in planning!

Additional tickets: \$125/pp

PRICING/ PACKAGE DETAILS

Book online: www.vanz.org.nz

* All prices exclude GST.

1 DAY

Tue 16th August 2022

Option 1

Practical Hands-on Awareness Day

Full day entry to the **Practical Hands-on Awareness Day**. See below for extra benefits (1).

\$200/pp

NO COST Offer! Open to students/apprentices and trainees with ID.

Full day entry to the **Practical Hands-on Awareness Day**. See below for additional benefits (1). Student ID Required.

FREE!

1 DAY

Tue 16th August 2022

Option 2

Asset Management/ Reliability Implementation Day

Full day entry to the **Asset Management/ Reliability Implementation Day**. See below for extra benefits (1).

\$350/pp

2 DAY

Wed 17th - Thur 18th August 2022

Main Conference

Conference attendance for two days. See below for additional benefits (2).

\$800/pp

HALF PRICE Offer! Open to students/apprentices and trainees with ID.

Full Day entry to the **Practical Hands-on Awareness Day**. See below for additional benefits (2). Student ID Required.

\$400/pp

3 DAY

Tue 16th - Thu 18th August 2022

Early Bird Pass!*

Full 3-Day Attendee

Full access to **Predictive Asset Management and Reliability Condition Monitoring Conference & Technology Exhibition**.

Conference attendance for three days. See below for additional benefits (2).

\$950/pp

pp = per person. * Early bird pass available until July 31st, 2022.

Additional benefits

1. Entry to the Awareness Day afternoon networking session.
All Awareness Day papers will be available to download from www.vanz.org.nz.
One day complimentary parking at the venue.
2. Complimentary parking at the venue.
All conference papers will be available to download from www.vanz.org.nz.
One year membership of VANZ included with attendance.

CONFERENCE '22

Wairakei Resort, Taupo: 16th – 18th August

Australasia's Premier Annual 3-Day Predictive Asset Management and Reliability Condition Monitoring Event.

'CONDITION MONITORING IN A CHANGING WORLD'

EXHIBITOR OPTIONS

* All prices exclude GST.

PACKAGE	Gold \$2,950	Silver \$2,100	Bronze \$1,480
Naming rights of conference			
Primary sponsorship on key online & offline promotional material before and during conference*			
Official role at the opening of the conference and five minute speaking opportunity			
Trade stand that offers sponsors the opportunity to showcase products, services and ideas	Premium	Standard	Table
Signage opportunities at conference & dinner			
Pre conference Spectrum advertising opportunities (early registrations only)	●		
Acknowledgement as sponsor & vendor	●	●	
Company literature in delegates goodie bags	●	●	
Brand on conference programme (early registrations 1 month before event)	●	●	●
Sponsorship on key online & offline promotional material before and during conference**	●	●	●
Logo on VANZ conference publications & website***	●	●	●
Post conference Spectrum advertising opportunities	●	●	
Conference entry for staff	x2	x1	x1

Booth size (Platinum and Gold)	1.8 x 3.0 metres
Booth size (Silver)	1.2 x 2.4 metres
Table top size (Bronze)	1.8 x 0.6 metres

Website* Animated landscape panels @ 460px wide x 200px high
Website** Animated landscape panels @ 460px wide x 200px high - x1
Logo file*** To be supplied as either a vector eps or hi res tif/png/jpeg

Files to be supplied to specifications.

ADDITIONAL SPONSOR OPTIONS AND INFORMATION

Lanyard sponsor	\$500 + lanyards
Bag sponsor	\$500 + bags
Dinner sponsor	POA
Informal Welcome Event (Tues night)	\$2,000

Need assistance?

For any enquiries, email
conference@vanz.org.nz,
 or visit our website: www.vanz.org.nz



Notice of AGM

DATE:

Thursday 18th August 2022

TIME:

9:30 to 10:10am

LOCATION:

Wairakei Resort Hotel - Stream Room 1

**Please attend if you can,
this association is run by you for you.**

Interested in joining

VANZ

Anyone with an interest in the area of mechanical and electrical machine condition monitoring, to facilitate predictive asset management is eligible to join VANZ.

In-house technicians, consulting engineers, suppliers and distributors of specialised equipment, engineering students can all contribute and gain from membership.

For more information about membership please contact the VANZ secretary by emailing secretary@vanz.org.nz





CONFERENCE TIMETABLE

Wairakei Resort, Taupo: 16th, 17th and 18th August 2022

'CONDITION MONITORING IN A CHANGING WORLD'

Tuesday 16th August - Day 1

Condition Monitoring Awareness stream plus Reliability Improvement stream

Start	Duration	End	
7:45 AM	0:45	8:30 AM	Registration and Exhibition / Trade Stand area is open for viewing, with Tea and Coffee available
8:30 AM	0:10	8:40 AM	Welcome to Conference 2022: VANZ President.
8:40 AM	0:10	8:50 AM	Overview of Conference Timetable for the Day and the next 2 days: Vice President.
8:50 AM	0:40	9:30 AM	Key Note Address: The 'Big picture' an Introduction into Condition Monitoring in a Changing World
9:30 AM	0:30	10:00 AM	Morning Tea in the Exhibition room / Trade Stand area (With Exhibitor introductions)
2 Streams; in Conference Rooms 1 and 2			The Tradesmans Tools' and installation specifications, to enable Predictive Asset Management
2 Hour - Asset Management and Reliability Program Implementation			
10:00 AM	0:15	10:15 AM	An 'overview' of today's sessions.
10:15 AM	0:30	10:45 AM	Install alignment -motor-coupling-gearbox-couplingpump hot and cold alignment. Commissioning new / refurbished installs to a specification.
10:45 AM	0:30	11:15 AM	Tribology Oil and Grease usage and practice. Commissioning new/ refurbished installs to a specification.
11:15 AM	0:30	11:45 AM	Basic vibration theory and practice. Commissioning baseline data to a specification.
11:45 AM	0:15	12:00 PM	Morning Sessions: Managed forum discussions.
12:00 PM	1:00	1:00 PM	Lunch in the Exhibition room / Trade Stand area
2 Streams; in Exhibition and Room 2			Electrical Machine Knowledge Exchange 'Hands-on' Condition Monitoring "Tools"
2 Hour - Asset Management and Reliability Program Implementation			
1:00 PM	0:45	1:45 PM	Practical tips for installing and operating electric motors.
1:45 PM	0:45	2:30 PM	Infrared and ultrasound usage and practice.
2:30 PM	0:30	3:00 PM	Lubrication: Oil and grease storage and application.
3:00 PM	0:30	3:30 PM	Afternoon Tea in the Exhibition room / Trade Stand area
3:30 PM	1:00	4:30 PM	Managed Forum Discussion Hands-On Demonstrations
			Round Table Discussions - Your chance to ask your questions from todays presenters, panel experts and colleagues on a specific subject at an assigned table.
4:30 PM	1:30	6:00 PM	'Meet & Greet' Networking Refreshments and Canapés available in the Exhibition Area that we encourage all to attend.

Wednesday 17th August - Day 2 - Main Conference

Start	Duration	End		
7:30 AM	0:30	8:00 AM	Registration and Exhibition / Trade Stand area is open for viewing, with Tea and Coffee available	
8:00 AM	0:10	8:10 AM	Welcome to Conference 2022 VANZ President.	
8:10 AM	0:10	8:20 AM	Official Conference Opening by the Conference sponsor -CSE W Arthur Fisher / Bruel & Kjaer Vibro.	
8:20 AM	0:45	9:05 AM	BK Vibro Key Note Address.	
9:05 AM	0:45	9:50 AM	Morning Tea in the Exhibitor room / Trade Stand area (With trade stand introductions)	
Two Streams of Presentations			Stream 1: Room One CM Technologies	Stream 2: Room Two Reliability based case histories
9:50 AM	0:40	10:30 AM	Mike Davis	TBC
10:30 AM	0:40	11:10 AM	Dr Iain Epps – Defect Severity Measurement in Rolling Element Bearings	TBC
11:10 AM	0:40	11:50 AM	Dare Petreski	TBC
11:50 AM	0:50	12:40 PM	Lunch in Exhibitor room / Trade Stand area	
Two Streams of Presentations			Stream 1: Room One CM based case histories	Stream 2: Room Two Reliability based case histories
12:40 PM	0:40	1:20PM	TBC	Colin Gracie – TBC
1:20 PM	0:40	2:00 PM	Mark Foster – Practical use cases for digital twin technology in asset reliability and condition monitoring	Matthew Fallow – The data was good/ Case history
2:00 PM	0:40	2:40PM	Stephen Reid/ GVS – Case History TBC	Craig Caryle – Effective Computerised Maintenance Management Systems
2:40 PM	0:30	3:10 PM	Afternoon Tea in the Exhibitor room / Trade Stand area	
3:10 PM	0:40	3:50 PM	James Neale – TBC	Michael Xu – Reliability
3:50 PM	0:40	4:30 PM	Bruce Shepherd – Case history TBC	Qing Ou – TBC
4:30 PM	1:30	6:00 PM	Complementary 'Meet & Greet' Networking Refreshments and Canapés available in the Exhibition Area that we encourage all to attend.	
7:00 PM	2:30	9:30 PM	Conference dinner	

Thursday 18th August - Day 3 - Main Conference **VANZ AGM will be held at 10:00 – PLEASE ATTEND!**

Start	Duration	End		
7:30 AM	0:30	8:00 AM	Exhibition room / Trade Stand area is open for viewing, with Tea and Coffee available	
8:00 AM	0:40	8:40 AM	John Van Zwiene: BK Vibro Key note Address	
8:40 AM	0:50	9:30 AM	Dare Petreski – TBC	
9:30 AM	0:40	10:10 AM	Morning Tea in Exhibitor area – VANZ AGM WILL BE HELD IN STREAM-1 ROOM –	
Two Streams of Presentations			Stream 1: Room One	Stream 2: Room Two
10:10 AM	0:40	10:50 AM	Simon Hurricks – Balancing Tips	Chris Pullen – TBC
10:50 AM	0:40	11:30 AM	Sven Fleisher – Alignment	CTC Rep – TBC
11:30 AM	0:40	12:10 PM	Les Pepper – The hydrogen scene in NZ	TBC
12:10 PM	0:50	1:00 PM	Lunch in the Exhibitor room / Trade Stand area	
1:00 PM	0:35	1:35 PM	Michael Eschenbruch – New technologies	
1:35 PM	0:35	2:10 PM	Craig Caryle – How to stay out of jail (What people are being prosecuted for)	
2:10 PM	0:35	2:45 PM	Dr Iain Epps – Influence of the Load Zone in Defect Severity Measurement	
2:45 PM	0:30	3:15 PM	Q&A session: Panel Q&A Discussions Your chance to ask any questions from all presenters, panel of experts and colleagues	
3:15 PM	0:15	3:30 PM	Awards Presentations, Vendor Prize Draws You need to be there to claim the prizes & Conference closing address	
Conference officially closed, we look forward to seeing you all again next year in 2023, at our 34th anniversary				

EDITORS' CORNER

Conference time (take 3) is back! We're going to try to have the event at the Wairakei Resort again as they have been gracious enough to help guide us through the pandemic with planning and regulations.

Our main sponsors for this year are CSE-W. Arthur Fisher representing BK Vibro and we are gearing up to put on the best possible conference we can for our patient delegates.

In this issue you can get your brain-pan popping with Carl's Quiz, read the latest Skills and Practices or muse over our President's pearls of wisdom.

Registration for conference v3.0 is available online at:



Many thanks to our advertisers who continue to support us these last couple years, not only through Spectrum but also with sponsorship at the conference and trade stands.

Happy Reading! ■



The AIP Value Cycle Proving that improvement pays

MOTION & CONTROL™
NSK

Partnering you towards machine optimisation

Our AIP Added Value Programme is based around a simple proposition: 'improvement pays'. By working with you throughout the AIP Value Cycle, we will help you achieve improvements in machine reliability, productivity and performance, all of which carry a tangible and measurable cost benefit – and we have the tools to prove it! That's what we mean by improvement pays.

The AIP programme comprises five clear steps which are called the Value Cycle:



A customized solution which identifies and quantifies the improvements and savings you'll make.

Rolling Bearings, Linear Technology and Steering Systems

NSK NEW ZEALAND

Add: Unit F, 70 Business Parade South, Highbrook Business Park, Auckland
Tel: +64 9 276 4992

Step 1 – Evaluation: We make site visits to gather data and understand the customers' challenges.

Step 2 – Recommendation: We use our learning, knowledge and experience to create a solution, including anticipated savings for the customer.

Step 3 – Implementation: We can assist, if required, with the installation and testing of our recommended solution and, if appropriate, we can also refine it for improved operation.

Step 4 – Validation: We monitor performance to ensure the anticipated results are being delivered.

Step 5 – Extension: We collate data, share learning and look to expand the service to new applications.

Gain an internationally recognised qualification in a growing area of industry.

Eurotec Thermography Certification Courses

Be sure. **testo**

optris
infrared measurements



EUROTEC People • Technology • Solutions
HVAC • Refrigeration • Electrical • Measurement

Your number one destination for thermal imaging products & services

Category 1 Thermography Certification Courses

15-19 August 2022, Auckland, New Plymouth & Christchurch

Learn how to use your thermal imaging camera to its full potential

Make use of all camera features and functions available for your specific application and gain a qualification at the same time!

Who is the course for?

Electricians, Insurance Reporters, Building Inspectors, Industrial Maintenance Inspectors, Inspectors of solar energy/ photovoltaic systems and more!



Scan to find out more

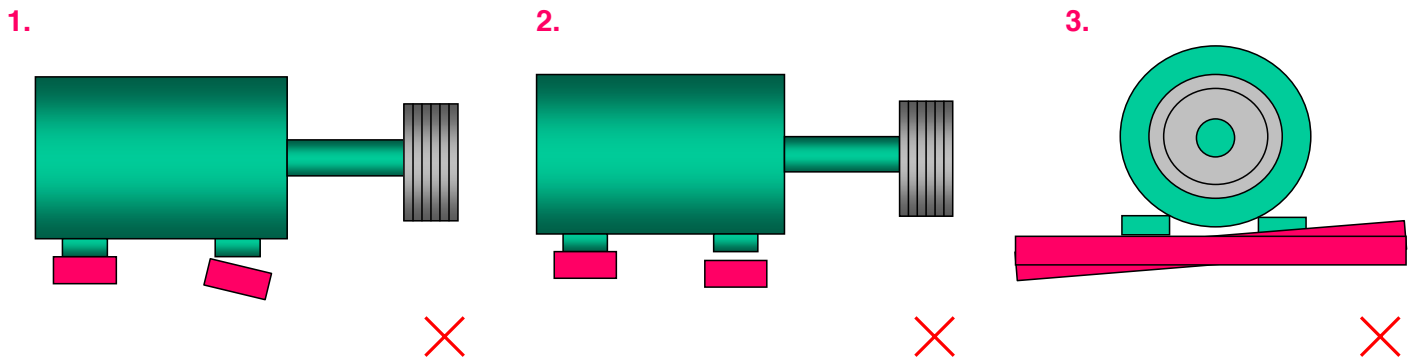
Contact us to book your seat!

www.eurotec.co.nz

09 579 1990

sales@eurotec.co.nz

SKILLS AND PRACTICES



SOFT FOOT on Belt Drive Motors...

We have seen in an earlier Flyer that “soft foot” is a condition that occurs when a machine or a component does not sit squarely and evenly on its mounting. This condition is bad for the machine because when you tighten the hold down bolt for the foot that is soft, the frame of the machine or component is distorted. This is a defect that reduces the life of the machine.

Electric motors in belt drive applications are often subject to soft foot.

The motor is mounted on slides that allow the motor to be moved backwards and forwards to adjust belt tension. It is essential that the faces of these two slides are in the same plane. If they are not, soft foot will result. This will cause high vibration levels and will shorten the life of the motor.

To get the slides in the same plane, it is necessary to shim the ends of the slides where they mount to their fabricated base. Use stainless steel shims. Bases are typically roughly fabricated and do not offer precise mounting of the slides.

Perform checks as shown in the illustrations:

1. Both slides must be parallel in line with motor axis.
2. Both slides must be at the same height.
3. Both slides must be parallel at right angles to the motor axis.

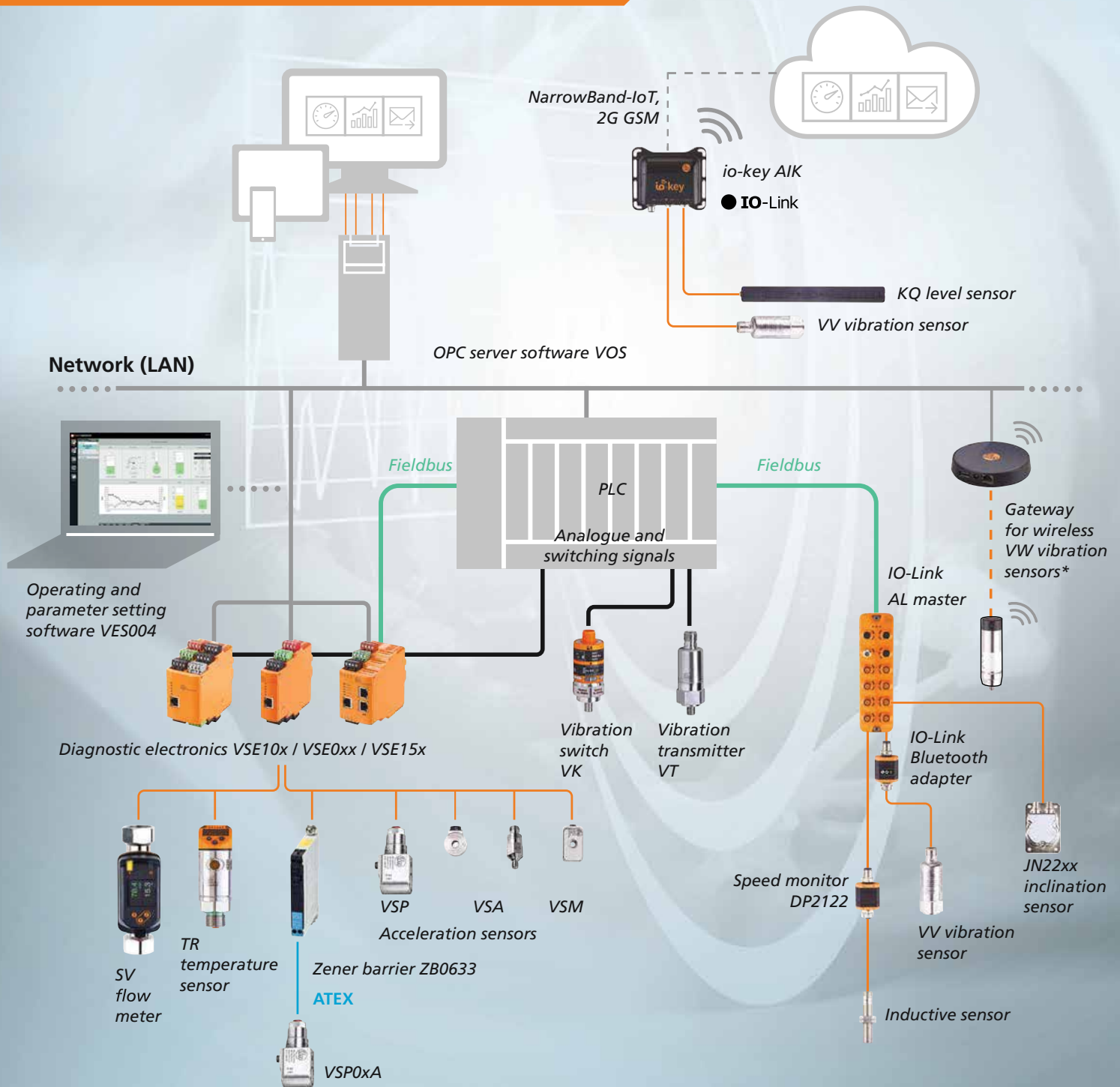
If these conditions are not met, then soft foot will result. The severity of the soft foot will also vary depending upon the position of the motor on the slides. ■



Plant Condition Monitoring Solutions



From Sensors to ERP



ifm offer a comprehensive range of industrial vibration and condition monitoring systems - ex-stock NZ! German quality - supported by local engineers, call us for advice on your machine requirements.

ifm – close to you!

www.ifm.com/nz ph: 0800 803 444

Vibration based condition monitoring of rotating part using spectrum analysis:

A case study on milling machine

1. Introduction

In the last few decades, industry concentrated on predictive maintenance rather than condition based maintenance and is practised still for the achievement of accurate fault diagnosis in machines. Many diagnosis strategies are being still explored by the researchers to diagnose and prognose the remaining useful life of machines. Condition Monitoring Sensor is a simple yet highly effective extension of all predictive maintenance. The sensor transmits all data into the software via Bluetooth, from which trend profiles and graphs can be analyzed. The industrial sector is in the midst of the biggest disruption in decades, causing players to face major pressures to become more reliable and productive while reducing costs. With the rapid changes that are happening in the market, organizations can no longer afford to continue to operate in a reactive environment, it's critical for organizations to reduce downtime, failure and production loss while extending equipment life and predicting expenditures – efficiencies that can transform operational costs. The adoption of efficient maintenance strategies is key to survival Condition-Based Maintenance and Predictive Maintenance are in almost every discussion that involves improving performance and reducing costs.

The Fault detection and identification of the machines are found by fault diagnosis method which plays a vital role for the maintenance of rotating machines. Also with the aid of vibration analysis the machine condition can be monitored constantly. Detailed analysis is used to find the machine health and fault identification may exist or arise.

2. Literature survey

Laxman Yadu et al., [1], paper describes the reliability analysis of cutting machine and also the life cycle cost estimation is predicted by the data collected from weibull software. After design changes reliability results increased from 15.85% to 22.09% of different machine components such as

bearing, control panel, pad, oil seal which is helpful for deciding interval maintenance. Mirghani N. Ahmed et al., [2], paper investigated on outsourcing of maintenance program with performance management and measurement system presents the risk of reliability of machines by the use of performance contract. This type of starting the program leads to the increase of financial benefit for the company and also qualitative products were achieved with the designed scheme.

Hooghoudt et al., [3], paper presents the effect made on capability improvement of bearings life and approaches towards the analysing of wear. A simulation model was developed for the data collection and monitoring from the signal analysis methods. The focus of this paper is on many evaluation procedures and to predict the remaining useful life of roller bearings. Yuri Merizalde et al., [4], paper reviews the online condition monitoring of wind turbines for the failure detection and diagnosis using signal analysis. The overall investigation for maintenance of wind turbines is analyzed by applying the current signature spectrum analysis. This work limits to the maintenance and further investigations on gearbox components.

3. Data collection from vibrometer device

Vibrometer is the first choice for non-permanent condition monitoring systems and it makes the process very simple and automated. It is ultra-portable and wireless. Additionally, it includes applications for mobile phones in case you want to work more comfortably. Fig. 1(a) and Fig. 1(b) shows of vibrometer cable and vibrometer instrument used in the present study for the data collection from the machines in three positions.

The specifications of Vibrometer are Measurement range are 2 mm/s to 5 m/s, Measurement frequency range is 1 Hz to 20 MHz, Velocity signal is ± 2.5 V (At input impedance 100 k Ω , output impedance 75 Ω , Power supply is AC 100 V to 240 V (50/60 Hz), 40 VA max.



Fig.1 (Above left). (a) Measurement cables; (b) Vibrometer instrument. **Fig.2 (Above right).** Class II level of Milling Machines.

4. Identification of critical part in Milling Machine

Milling machine major parameters include the depth of cut, feed rate and speed of the shaft. The below Fig. 2 represents the severity of critical machine which has high level of vibration and designated as Class II machines.

The standard level of Class II machines is decided due to the range of 2.1 m/s to 7.1 m/s. The specifications of the milling machine having table size 260x1200mm, travels of 675x440x340mm, power feed of 640 m/s, rotate parallel having 360, motor power of 3 HP. Machine found to be having higher level of vibration during operation.

5. Graphical analysis of Motor drive spectrums

Fig. 3 represents the peak value of 0.4 m/s and 0.38 m/s velocity at 100 Hz frequency before and after replacement of components which are analyzed by spectrums and proper diagnosis is suggested for the machine to increase the production rate and accuracy. The graph illustrations on the following page are drawn using Origin tool and obtained from vibrometer instrument directly by which data collected and analyzed for the purpose of efficient performance of machines leads to increase in accuracy. Fig. 4 shows the vibration severity of

machines as per ISO 10,816 and it indicates velocity.

6. Conclusion

This paper gives the brief of device fault detection, diagnosis, and diagnosis of the rolling bearing and also describes the liberation size of the wavelet thru the machine factors. Paper presents the maximum important technology or methodology of fault detection, analysis, and diagnosis respectively. Subsequently, segment five offers a few conclusions and states new challenges. Data were collected using Vibrometer instrument and readings are analysed using signal processing techniques to check the severity level of the rotating machines. As shown in this paper spectrum analysis strategies for fault detection and prognosis have been investigated which will clear up this trouble.

Declaration of Competing Interest

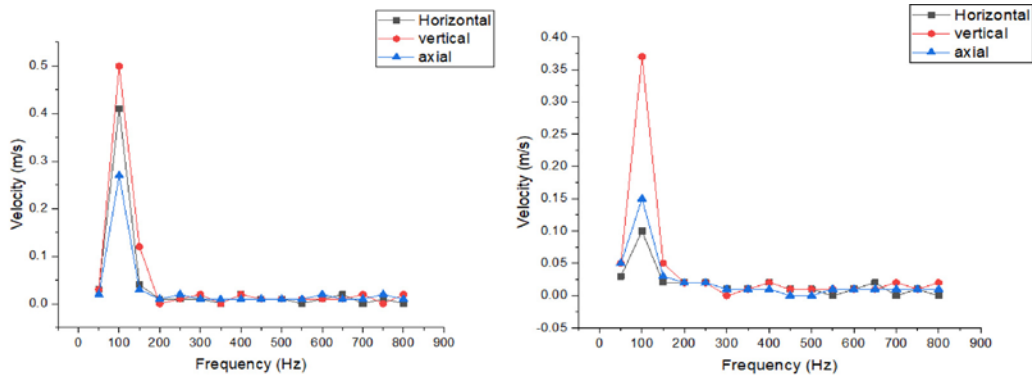
The authors declare that they have no known competing financial interests or personal relationships that could have appeared to influence the work reported in this paper. ■

Continued over page >

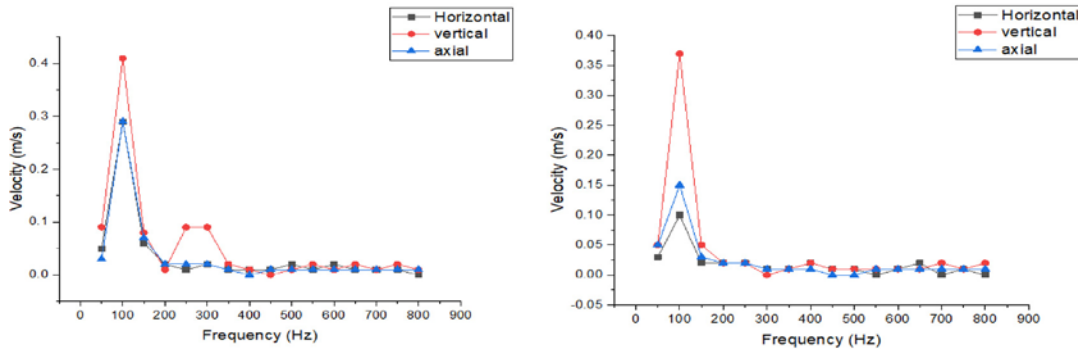
DID YOU REGISTER FOR THE VANZ 2021 CONFERENCE LAST YEAR?

You and your business may be eligible for a **15% discount on 2022 prices.** Enter your unique code at www.vanz.org.nz to take advantage of this special offer!





(a) Motor drive readings on Mar 2019; (b) Motor drive readings on Aug 2019



(c) Motor drive readings on Mar 2020; (d) Motor drive readings on Aug 2020

Fig.3 (Above). (a) Motor drive readings on Mar 2019; (b) Motor drive readings on Aug 2019; (c) Motor drive readings on Mar 2020; (d) Motor drive readings on Aug 2020.

Fig.4 (Right). Vibration velocity values for different classes.

VIBRATION SEVERITY PER ISO 10816					
Machine		Class I small machines	Class II medium machines	Class III large rigid foundation	Class IV large soft foundation
Vibration Velocity Vrms	in/s	mm/s			
	0.01	0.28			
	0.02	0.45			
	0.03	0.71		good	
	0.04	1.12			
	0.07	1.80			
	0.11	2.80		satisfactory	
	0.18	4.50			
	0.28	7.10		unsatisfactory	
	0.44	11.2			
	0.70	18.0			
0.71	28.0		unacceptable		
1.10	45.0				

References

- [1] L. Yadu, R. Patil, Reliability analysis and life cycle cost optimization: a case study from Indian industry, Journal of Reliability paper, Annaseb college og Engineering, Asta, India, 2016, pp 1-9.
- [2] M.A. Ahmed, The use of performance-based contracting in managing the outsourcing of a reliability-centered maintenance program A case study, Emerald insight, journal of quality of maintenance, ISSN 1355- 2511, 2019, pages 1 – 29.
- [3] J. Hooghoudt, Y. Otto, Predicting the remaining useful life of rolling element bearings, Aalborg University, Denmark, 2018, pages 9-17.
- [4] Y. Merizalde, S.N. Verma, A.K. Wadhvani, Application of ANN, fuzzy logic and wavelet transform in machine fault diagnosis using vibration signal analysis, Journal of Quality in Maintenance Engineering, Emerald Group Publishing Limited, ISSN:1355-2511, Vol. 16 No. 2, 2010.
- [5] Monash University, Clayton, VIC 3800, Australia 2016, pages: 638–651.
- [6] L.H. Callejo, O.D. Perez, Diagnosis of wind turbine faults using generator current signature analysis: a review, Journal of Quality in Maintenance Engineering, Emerald Publishing Limited, Vol.26, No.3, 2020, ISSN: 1355-2511, pages. 431-458.
- [7] K. Droder, W. Hoffmeistera, M. Luiga, T. Tounsi, Real-time monitoring of highspeed spindle operations using infrared data transmission, International Conference on Performance Cutting, Germany, 2014, 488 – 493.
- [8] N. Jamaludin, D. Mba, R.H. Bannister, Condition Monitoring of slow-speed rolling element bearings using stress waves, J. Eng. 215 (4) (2001) 245–271.
- [9] A.T. Hiroshi, Application of condition monitoring system for wind turbines, New Energy Engineering Department Industrial Machinery Division, TECHNICAL REVIEW No.80, 2012.
- [10] A.A. Mohamed, R. Neilson, P. Mac Connell, Monitoring of fatigue crack stages in a high carbon steel rotating shaft using vibration, University of Aberdeen, UK, Procedia Engineering 10 (2012) 130–135.
- [11] C. Zhao, Y. Chen, H. Wang, H. Xiong, Reliability analysis of aircraft condition monitoring network using an enhanced BDD algorithm, School of Electronics and Information Engineering, Beihang University, Beijing,2012, china, 925-930.
- [12] S. Sheng, Wind turbine gearbox condition monitoring – vibration analysis, Applied Systems Health Management Conference, Virginia, 2011.

Further Reading

- [1] J.P. Patel, S.H. Upadhyay, Comparison between artificial neural network and support vector method for a fault diagnostics in rolling element bearings, 12th International Conference on Vibration Problems, ICOVP 2015, Science Direct, Procedia Engineering 144, (2016), pages 390 – 397.
- [2] Md. Mamunur Rashid, M. Amar, I. Gondal, J. Kamruzzaman, A data mining approach for machine fault diagnosis based on associated frequency patterns, Springer Science+Business Media New York,



CONDITION MONITORING WITHOUT SENSORS

The AMT Pro provides:

- Model based fault diagnosis technology
- Detects mechanical faults, electrical faults and process faults
- Portable or online

Visit our stand for a demonstration of the AMT Pro.

NVMS 

+64 274 664 810

nvms.co.nz

Effect of Vibration and Noise Measuring Points Distribution on the

Sensitivity of Pump Cavitation Diagnosis

Cavitation is an essential factor in the deterioration of the hydraulic performance of centrifugal pumps. The study of cavitation fault diagnosis can help prevent or reduce the damage it causes. The vibration and noise analysis method can predict the incipient cavitation more accurately. In order to improve the accuracy of cavitation fault diagnosis, this paper studied the sensitivity of measuring points distribution for centrifugal pump cavitation diagnosis. The research object is a centrifugal pump with an inducer and splitter blades. Vibration acceleration sensors and hydrophones were used to collect structural vibration and liquid-borne noise signals at different positions of the pump unit. Root-mean-square (RMS) and fast Fourier transform (FFT) methods were used to construct spectrums of vibration and noise signals with different NPSHa and compare the sensitivity of different measuring points to the inception and development of cavitation. In addition, the SST k - ω turbulence model and Zwart cavitation model were used to study the cavitation volume distribution in the pump under different cavitation stages. By setting monitoring points at the impeller outlet, the frequency domain signal distribution of pressure pulsation was studied. The results show that the vibration measuring points at the inlet flange and pump axial position (increased by about 0.6 % at NPSHr) and liquid-borne noise measuring point at the inlet position (reduced by about 14 % at NPSHr) are more sensitive to the diagnosis of cavitation fault. Motor current is also the basis for judging the inception of cavitation. When severe cavitation occurs, the current drops sharply by approximately 12 %. Moreover, the pressure pulsation intensity at the inlet decreases by 66.3 % and by increases 13.9 % at the outlet, respectively, with a 3 % drop in head. As the cavitation intensifies, the dominant frequency of the pressure pulsation in the pump is partially shifted. The presented results indicate the distribution of measuring points with good sensitivity, providing a reference for improving the accuracy and efficiency of cavitation predictions for centrifugal pumps.

Introduction

Cavitation affects the operational stability and efficiency of the pump and is an essential indicator of pump performance. Generally, cavitation occurs when the absolute static pressure at the pump inlet is below the saturation vapor pressure, resulting in a disturbance and disruption of the energy exchange between the impeller and the liquid, and a significant reduction in the external characteristic curve. In severe cases, the liquid flow in the pump can be interrupted, causing the pump not to operate properly. The bubbles are transported to the high-pressure area and ruptured in a very short time, generating massive shock waves.

The rupture of the bubbles causes severe damage to the impeller surface material in the form of pitting and erosion, resulting in the pump producing vibration and noise [1]. It is not possible to suppress

Cavitation is an essential factor in the deterioration of the hydraulic performance of centrifugal pumps.

cavitation completely. Therefore, to ensure the reliability of pump operation, it is necessary to accurately detect the onset and development of cavitation, and control the operating conditions to prevent cavitation. The development of cavitation is mainly divided into the inception, development, and degradation stages [2] to [5]. During the different stages of cavitation, there are variations in the quantities of pressure, flow rate and motor power. These features can be used to diagnose the severity of cavitation.

The net positive suction head (NPSH) is commonly used in engineering to determine the operating conditions and suction performance. According to the ISO 3555 standard [6], the NPSH value for a 3 % drop in the total delivery head is defined as NPSH-required (NPSHr), representing cavitation that has fully developed.

Continued over page >

NEW PRODUCT ALERT:



Easy Bar® with Almasol® (9210)

A solid lubricant that melts when placed on the hot surface of a kiln shell. It features a patented blend of mineral and metal lubricants – including Almasol, LE's proprietary solid wear-reducing additive suspended in a solid polymer binder that melts at approximately 49°C.

Typical Applications:

- Rotary Kilns, Dryers, Calciners,
- Cement, Lime, Pulp & Paper, Waste Processing
- Mining & Phosphate, Petroleum & Asphalt, Minerals
- Chemical, Food & beverage, Gypsum, Clay & Kaolin
- Iron ore & Aluminum



Lubricant Bar Effectiveness

Lubricant bars are solid dry lubricants encased within a carrier agent, which can be wax, polymer or other compound. This agent generally has a melting point of less than 93°C (200°F) and, when placed adjacent to the heated kiln shell, melts and releases the lubricant. Turning of the kiln causes these lubricants to flow over the wear pads and inside the tire bore, coating the mating surfaces.

Lubrication of the entire inside tire bore is crucial for effective lubrication. Solid bar lubrication between the filler bars or kiln shell and riding rings of a rotary kiln is proven to:

- Extend the life of wear filler bars
- Extend shell and refractory service life
- Reduce scoring of kiln tires, inside bore, riding rings, and stop blocks
- Reduce weld fractures at filler bar and kiln shell interface
- Reduce friction and wear
- Fill microscopic imperfections in contact surfaces

Lubricant Bar Application

Safe, Efficient Bar Insertion

While the kiln rotates, the operator simply inserts the recommended number of lube bars in the filler bar gaps between the tire and the shell. Insertion involves placing a whole bar between the filler bars or pads at the 5 or 7 o'clock positions. This should be done every quarter turn of the kiln as it travels through one full revolution.



For further information go to www.lubricationengineers.co.nz or Call Chris 021 385 487

When the cavitation occurs, it causes a change in pump load torque. The electric signal in the motor can evaluate the impeller torque, which can detect the beginning of cavitation. Meanwhile, cavitation can be predicted by measuring the line voltage and phase current on the power transformer [7] and [8].

The normalized amplitude at the third-order rotational speed obtained by measuring the instantaneous angular velocity of the pump and the order spectrum analysis can also be used for characteristic monitoring [9]. Vibration and noise are generated due to the continuous rupture of the bubbles in the high-pressure region accompanied by strong water shock during vapourization inside the pump. There is a discrete frequency or broadband peak in the audible noise spectrum, which is closely related to the development of cavitation. The discrete frequencies are consistent with the NPSHr, and both can correspond to a 3 % drop in the total delivery head. The characteristic discrete frequency tones closely associated with cavitation are the resonance caused by structural vibrations or the rupture of bubbles on the inner wall surface of the pump, so the discrete frequency tones can detect the intensity of cavitation. The measurement methods are mainly divided into three types: sound pressure level in air, underwater acoustics and structural vibration [10] to [12]. Černetič [13] and Černetič and Čudina [14] evaluated the uncertainty of cavitation prediction for vibration and noise signals from centrifugal pumps in broad frequency range and at discrete frequencies, verifying that vibration and noise in the audible frequency range are capable of predicting and diagnosing cavitation.

Chini et al. [15] analysed the noise spectrum of centrifugal pumps to find the feature of cavitation initiation and found that sound pressure levels at some frequencies can detect the inception of cavitation and quantify the severity of cavitation. Wang et al. [16] found that as cavitation intensifies, the vibration acceleration and noise stabilize at first and then increase apparently, which can determine the NPSH-inception of the pump. Zhang et al. [17] found that the cavitation critical point inferred from the vibration level is higher than the NPSHr when the head drops by 3 %, indicating the actual cavitation time is earlier than that reflected by the head curve. Dong et al. [18] found that with the decrease of NPSH, the total sound pressure level of liquid-borne noise first increase and then decreases, and the sound pressure level of liquid-borne noise in the 2 kHz to 3 kHz frequency range can better predict the initiation of cavitation, with a threshold value of 1 %. Al-Obaidi [19] to [22] used time-domain analysis (TDA) and fast Fourier transform (FFT) techniques for frequency domain analysis (FDA) based on vibration and acoustic analysis methods.

The ability of the different methods to diagnose pump cavitation under different operating conditions was compared and evaluated, proposing that peak and peak-to-peak values are more sensitive to cavitation detection in pumps than the RMS and variance feature. Mousmoulis et al. [23] concluded that the impeller's geometric parameters affect the development of cavitation, and that acoustic and vibration measurements can effectively predict cavitation.

Many researchers have asserted that the signal features of vibration, noise, and pressure pulsation can effectively predict the initiation and development of pump cavitation, and proposed signal processing and analysis methods to detect cavitation. However, there is a lack of studies on the sensitivity of measuring point distribution for cavitation prediction. In practice, the characteristics of the vibration signal at different positions are dissimilar. And the liquid-borne noise and pressure pulsation characteristics of the inlet and outlet have different sensitivities to cavitation prediction. Therefore, the location of the measuring points has a crucial influence on the accuracy of cavitation fault diagnosis. To improve the prediction of cavitation and reduce the damage to the pump, it is necessary to research the effect of measuring point distribution on cavitation fault diagnosis.

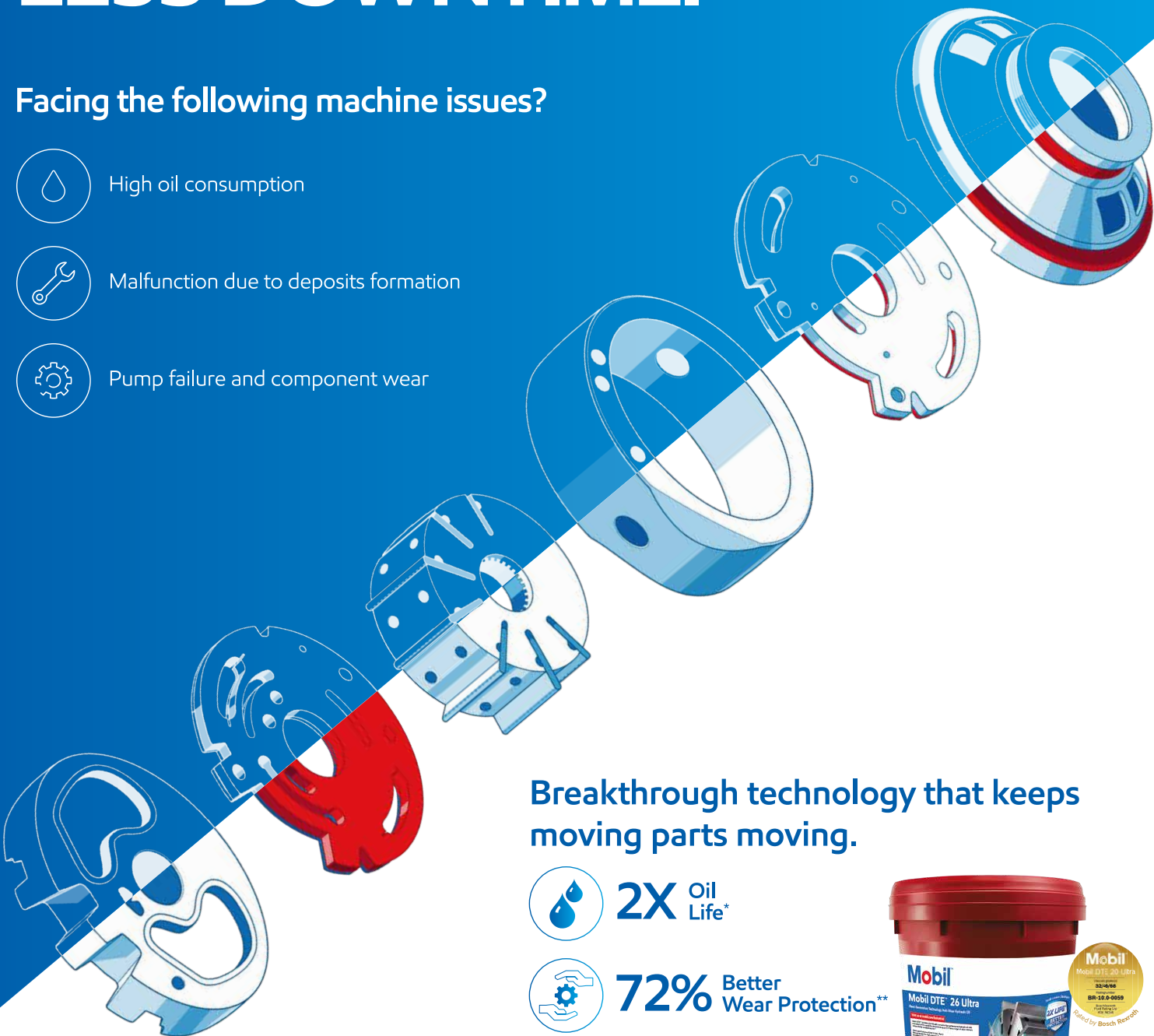
In the actual operation of the pump, the flow rate is reduced due to the influence of cavitation. In some special applications, there are high demands on the stability of the pump flow rate, for example, fuel pumps for the liquid rocket engine. The cavitation test is usually carried out by keeping the flow rate at a constant value [24], which can intuitively evaluate the cavitation performance of the centrifugal pump. However, it cannot restore the actual situation properly. This paper took a small flow rate and high head centrifugal pump with an inducer and splitter blades as the research object. The valve opening was constant during the cavitation test so that the flow rate varied continuously with the development of cavitation. In addition, hydrophones and high-frequency pressure sensors were installed at the inlet and outlet, and eight vibration sensors were installed at the inlet and outlet flanges, the pump axial and radial, the pump foot, and the bearing housing. The signal characteristics at different locations under different cavitation conditions were measured. The sensitivity of different measuring points was analysed to obtain the optimum method for detecting the onset and development of cavitation in centrifugal pumps and improving the accuracy of cavitation fault diagnosis in centrifugal pumps.

Continued over page >

IT'S TIME FOR LESS DOWNTIME.

Facing the following machine issues?

-  High oil consumption
-  Malfunction due to deposits formation
-  Pump failure and component wear



Breakthrough technology that keeps moving parts moving.

-  **2X** Oil Life*
-  **72%** Better Wear Protection**
-  **89%** Better Deposit Control*



MOBIL DTE™ 20 ULTRA SERIES

Decreased downtime with extended:

- Component life
- Oil drain intervals
- Filter life

Disclaimer: *Mobil DTE 20 Ultra Series oils have demonstrated up to 2 times longer oil drain intervals versus similar competitive oils (ISO VG 46 with a viscosity index around 100 and a zinc-based anti-wear system - meeting at least ISO 11158 (L-HM) and/or DIN 51542-2 (HLP type) requirements) in demanding Mobil Hydraulic Fluid Durability (MHFD) testing. **72% lower wear than maximum limit for motor wear in BR RFT APU CL test (ISO VG 32). *89.2% lower sludge formation than maximum limit of ASTM D 6158 by using ASTM D 2070 method (ISO VG 68).

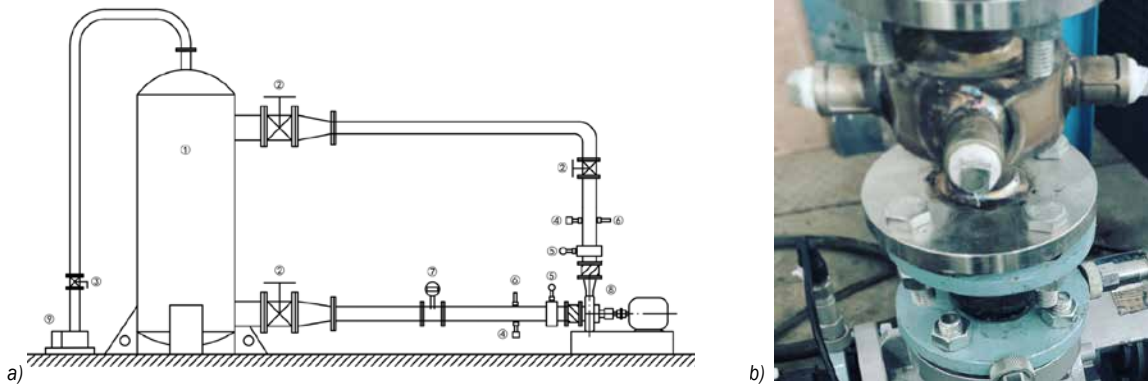


Fig. 1. Centrifugal pump cavitation test bench; a) test bench (1. cavitation tank, 2. gate valve, 3. ball valve, 4. pressure pulsation sensor, 5. pressure transmitter, 6. hydrophone, 7. electromagnetic flowmeters, 8. pump set, 9. vacuum pump), and b) vibration measuring points.

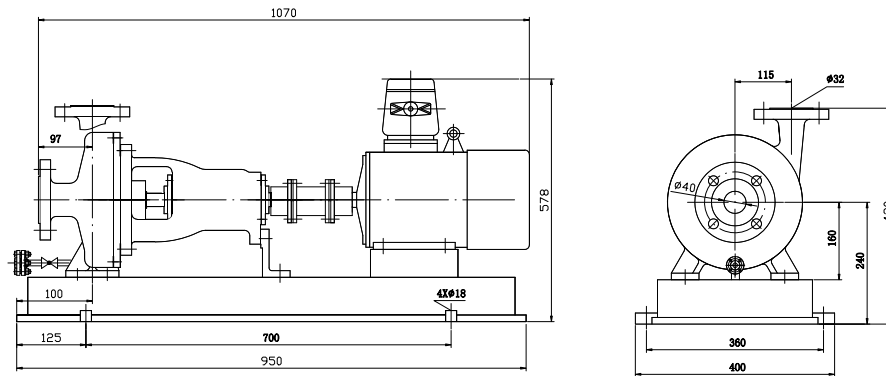


Fig. 2. Two-dimensional structure of test pump.

1. Test and Simulation Methods

1.1 Research Object

The test bench comprises a vibration and noise high-frequency signal test system, an external characteristic test system and a data acquisition system.

Fig. 1a shows that the test equipment includes a cavitation tank, a vacuum pump, pipelines, valves, an electromagnetic flowmeter, test pumps, motors, pressure transmitters, hydrophones, vibration acceleration sensors, and pressure pulsation sensors. The pressure transmitters are located at two times the pipe diameter of the pump inlet and outlet flange. The hydrophones and pressure pulsation sensors are installed eight times the pipe diameter. Moreover, the vibration acceleration sensors are installed in eight positions: inlet flange vertical and horizontal, outlet flange vertical and axial, pump body radial, axial and foot, and the bearing house, as shown in Fig. 1b. A small flow rate and high head centrifugal pump with a specific speed of 25 was used as the research object, and the equation for the specific speed is as follows [1]:

$$n_s = \frac{3.65n\sqrt{Q}}{H^{3/4}}. \quad (1)$$

The design parameters of the pump are flow rate $Q_d = 5 \text{ m}^3/\text{h}$, head $H_d = 39 \text{ m}$, and rotational speed $n = 2900 \text{ r/min}$. The centrifugal pump impeller has four main blades and four splitter blades, the diameter of the impeller $D_j = 160 \text{ mm}$, the outlet width of the impeller $b_2 = 6.5 \text{ mm}$, and the blade wrap angle $\phi = 80^\circ$. The inducer has a tapered hub with equal pitch double blades. The axial length of the hub is $h_h = 40 \text{ mm}$, the axial length of the rim $h_y = 30 \text{ mm}$, and the inlet sweep angle $\theta_r = 140^\circ$. The structure of the test pump is shown in Fig. 2.

1.2 Test Method

The centrifugal pump cavitation tests are usually carried out at a constant flow rate [1], which means that the outlet valve is controlled to keep the flow rate unchanged. The pressure at the inlet is reduced by a vacuum pump, causing the pump to cavitate. This method can effectively obtain the cavitation performance curve of the pump at a fixed flow rate. However, in many practical applications, it is impossible to adjust the valve in time to keep the flow rate constant. The flow rate decreases with the intensification of cavitation and even breaks down. For example, the heavy drop in flow rate caused by cavitation can result in the turbopump being unable to supply oxidizer to the liquid rocket engine in time,

leading to severe operational failure of the rocket. Very few cavitation tests with a fixed valve have been carried out, specifically with the flow rate changes as cavitation. Therefore, this paper used this method to conduct cavitation tests and measured pressure pulsation, vibration and noise signals. The vibration and noise signal under cavitation is significantly different from other mechanical faults in terms of spectral distribution. The broadband character of cavitation has an effect not only on low-frequency signals but also on the higher frequency bands [25]. According to the Nyquist-Shannon sampling theorem, the sampling frequency is more than twice the highest frequency in the signal, so that the information in the original signal is not lost from the acquired digital signal. In order to make the acquired signal reflect the trend in the high-frequency band and ensure the accuracy in the low-frequency band, a sampling frequency of 10 kHz is used to acquire the signal, considering the sensors' operating range and each sampling time is 3 s. And the test steps are as follows.

1. Adjust the pump motor speed to 2900 rpm by frequency converter.
2. Control the outlet valve to stabilise the initial flow rate at 5 m³/h.
3. Turn on the vacuum pump and reduce the inlet pressure of the centrifugal pump.
4. Obtain signals for flow rate, pressure pulsation, liquid load noise and structural vibration at different NPSHa.

The data were processed and analysed using MATLAB software. The vibration and noise signals are processed as follows:

(1) Vibration acceleration levels

The intensity of vibration (i.e. the energy of vibration), is commonly expressed by physical quantities such as velocity, acceleration and displacement. In contrast, acceleration can better reflect the impact of vibration on the structure. Therefore, the RMS value of acceleration is generally used to express the intensity of the vibration. In practice, the vibration is compound: not a single frequency vibration but superimposed vibrations of multiple frequencies. For evaluating vibration energy, one of the commonly used evaluation indicators is vibration acceleration level. The vibration acceleration level VAL is defined as [26]:

$$VAL = 20 \lg(a_r / a_0), \quad (2)$$

where a_r is the RMS of acceleration, and a_0 is the reference acceleration, generally $a_0 = 10^{-6} \text{ m/s}^2$. The unit of vibration acceleration level is decibel, [dB]. And the RMS of vibration acceleration a_r defined as follows [26]:

$$a_r = \sqrt{\frac{1}{T} \int_0^T a_i^2(t) dt}, \quad (3)$$

where $a_i(t)$ is the acceleration at some point, and T is the total number of samples.

(2) Sound pressure level

The hydrophone is affected by the hydroacoustic sound pressure P in the sound field, which generates an open-circuit voltage U . The open-circuit voltage U is proportional to the sound pressure P . Therefore, the hydrophone sensitivity M can be obtained as [27]:

$$M = U / P, \quad (4)$$

where U is usually defined as the open-circuit voltage generated when the hydrophone is subjected to 1 Pa liquid-borne sound pressure in the sound field. The sensitivity is compared with the reference value and then taken logarithmically to obtain its corresponding decibel value. In hydroacoustics, 1 μPa is usually used as the sensitivity reference. The output voltage signal of the hydrophone is processed by the FFT method to obtain the voltage spectrum and logarithmically transform the voltage spectrum to obtain the voltage decibel [27]:

$$U_{dB}(f) = 10 \lg(U_{FFT}(f)), \quad (5)$$

where $U_{FFT}(f)$ is the amplitude of the hydrophone's voltage spectrum at some frequency. The sound pressure level of the liquid-borne noise at this frequency is obtained by subtracting the voltage decibel from the sensitivity of the hydrophone [27]:

$$SPL = U_{dB}(f) - M(f). \quad (6)$$

Similar to the total vibration level calculation, the total sound pressure level of liquid-borne noise is calculated as follows [27]:

$$SPL_t = 20 \lg(p / p_{ref}), \quad (7)$$

where p is the RMS of sound pressure, and p_{ref} is the reference value of underwater sound pressure, 1 μPa .

1.3 Numerical Simulation Method

Creo 5.0 was used to build the 3D model of the pump. The entire model was divided into five parts: the inlet pipe, the inducer, the impeller, the volute and the outlet pipe. ANSYS-ICEM 17.0 was adopted to generate tetrahedral grids, as shown in Fig. 3. To meet the requirements of numerical simulation on grid quality, the grids around the volute tongue and blades are improved and smoothed. The average y+ of the grid model is less than 80. Five sets of grids with different cell numbers were generated to verify the grid independence, as listed in Table 1. The judgment basis was that head error of less than 1 % and the time cost of the calculation is as short as possible. The second grid set is closer to the actual parameters in terms of head and has fewer cells than the other sets.

Continued over page >

Table 1. Grid independence verification.

Program	Inlet and outlet section	Volute	Inducer	Impeller	Total	Head [m]	Error [%]
1			1.18×10^6	1.53×10^6	4.11×10^6	39.18	0.46
2			9.22×10^5	1.04×10^6	3.37×10^6	39.14	0.35
3	6.42×10^5	7.61×10^5	7.81×10^5	9.43×10^5	3.13×10^6	39.31	0.79
4			6.21×10^5	8.21×10^5	2.85×10^6	40.26	3.23
5			5.35×10^5	7.43×10^5	2.68×10^6	40.32	3.49

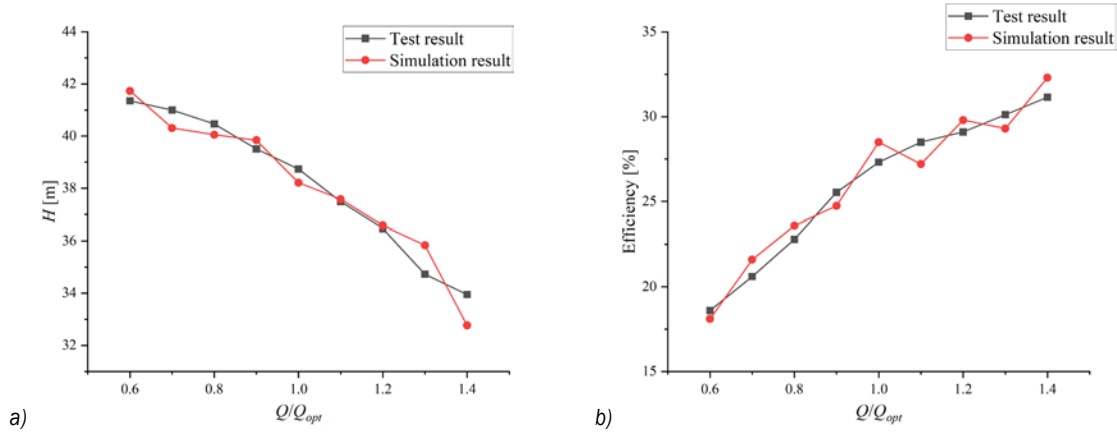
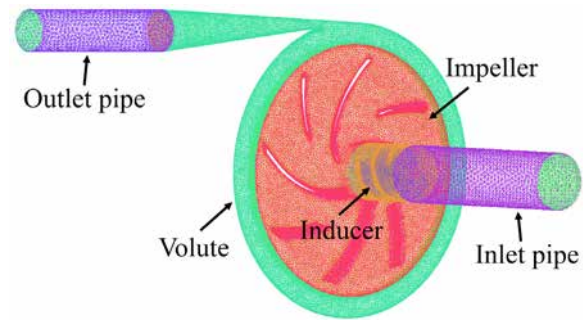


Fig. 4. Comparison between simulation results and test results, a) Q-H curve, and b) Q-Efficiency curve. **Fig. 3 (Below).** Grid model.

Therefore, this paper used this grid for numerical simulation. Fig. 4 compares the external characteristic results of the numerical simulation with the test. The trend of the numerical simulation and the test result is the same. As the flow rate increases, the head of the centrifugal pump trends to decrease, and the efficiency increase significantly. The head and efficiency at each operating point obtained by the numerical simulation are consistent with the test results, and the maximum error does not exceed 3 %. Therefore, the numerical simulation results have good accuracy.

The ANSYS-CFX17.0 software was applied to numerically simulate the cavitation of a centrifugal pump at different inlet pressures. The pump's inlet and outlet boundary conditions were set according to the inlet pressure and the flow rate results obtained by the test at different NPSHa. The evolutions of the internal flow field and vapour volume under different cavitation stages were obtained through numerical simulation. The turbulence model uses the shear stress transport $k - \omega$ (SST $k - \omega$). This model is widely used in rotating machinery [28]. The SST $k - \omega$ can better calculate the adverse pressure gradient and separation flow. It predicts the pump's performance more accurately [5]. The rotor-stator interfaces use the transient rotor-stator. The pitch change is specified pitch angles with a value of 360° , and the interface between the impeller and the inducer is relatively stationary. The grid connection between the interfaces is set as the general grid interface (GGI). The fixed wall adopts no-slip, and the rotating walls on the impeller and inducer are moving walls. The advection scheme adopts the high resolution, and the transient



scheme adopts the second-order backward Euler. The maximum number of inner iteration loops is set to 20. The residual accuracy was $10e-4$. The rotational speed is 2900 rpm. The time step is the time taken for each 2° rotation of the impeller, i.e. 0.0001494 s. The total time step is the time taken for five cycles of the impeller. The steady-state results are taken as the initial values for the unsteady-state calculations. The fluid medium is water at 25°C . The gas medium is set to water vapour at 25°C , the Saturation Pressure of the fluid is 3169 Pa, the reference pressure is 0 Pa, the volume fraction of the inlet vapour is set to 0, and the volume fraction of the liquid is set to 1. The Zwart cavitation model is used. The net positive suction head available (NPSHa) of the pump is calculated as [1]:

$$NPSHa = \frac{P_s - P_v}{\rho g} + \frac{v_s^2}{2g}, \quad (8)$$

where P_s is the pump inlet pressure; P_v is the saturated vapour pressure of the fluid at operating temperature; v_s is the flow rate at the pump inlet.

Continued over page >

EagleBurgmann®

Rely on excellence



Made to meet your need,
but exceed your expectations

- Mechanical Seals • Cartridge Seals
- Seal Supply Systems • Gland Packing
- Static—Sheet Jointing / Formed Gaskets
- Expansion Joints—Fabric / Rubber / Metal
- Bearing Isolators • Current Diverter Rings
- Couplings—Diaphragm / Magnetic
- Marine Seals • MECO Seals
- Dry Powder Seals • Segmented Carbon Rings



EagleBurgmann Australasia Pty Ltd (NZ)

PO Box 300858, Albany, Auckland 0752, 47 William Pickering Drive, Rosedale, Auckland 0632
Ph: +64 (0)9 448 5001, Fax: +64 (0)9 415 0599, Email: sales@nz.eagleburgmann.com

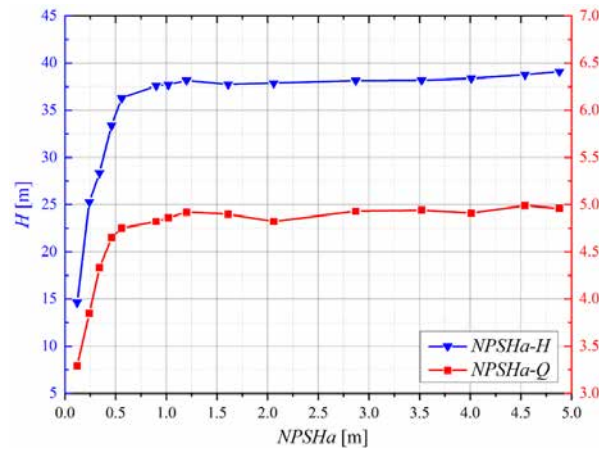
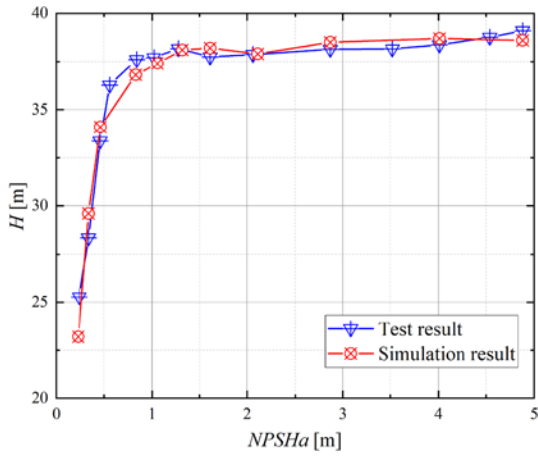


Fig. 5 (left). Comparison of cavitation performance curves. **Fig. 6 (right).** Variation of head and flow rate with NPSHa.

Fig. 5 shows the cavitation performance curves obtained from the tests and numerical simulations. The trends in the cavitation performance curves are generally consistent, although there are some errors between the simulation and test results. The inception points of cavitation in test and simulation are almost the same. The NPSHr measured by the test is 1.03 m, while the simulation result is 1.06 m, with an error of about 3 %. When the head drops by 10 %, the NPSHa values of both are also very close. Therefore, the simulation results can more accurately reflect the evolution of cavitation.

2. Analysis of Cavitation Prediction Methods

2.1 External Characteristics

Fig. 6 shows the flow rate and head variation curves for different NPSHa obtained from cavitation test with fixed valve. A slight drop in the head occurs as the NPSHa decreases from 5 m to 2 m. At NPSHa = 3.83 m, the head drops by approximately 1 %. There is some fluctuation in flow rate but no significant drop. When NPSHa reduces from 2 m to 1.5 m, the head and flow rate both decrease first and then rise. With the decrease of NPSHa (1.5 m to 0.5 m), cavitation in the pump begins to develop continuously, and the

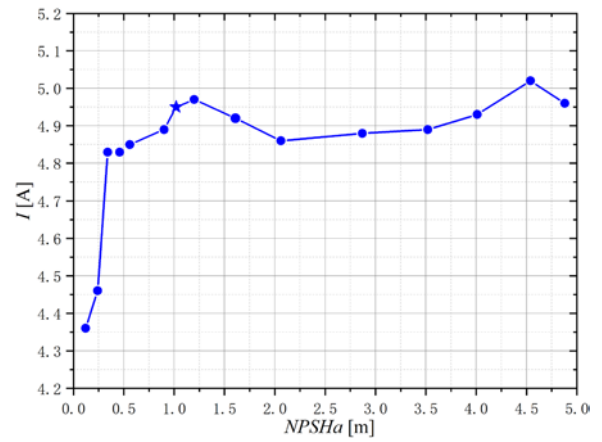


Fig. 7. Variation of motor current with NPSHa.

head and flow rate decrease again. When NPSHa = 1.02 m, the head drops by 3 %, which is the net positive suction head required (NPSHr), meaning that full cavitation has occurred at this time [6]. Cavitation continues to intensify after the NPSHa falls below 0.5 m. The flow rate and head drop drastically, and the pump has a significant loss of hydraulic performance.

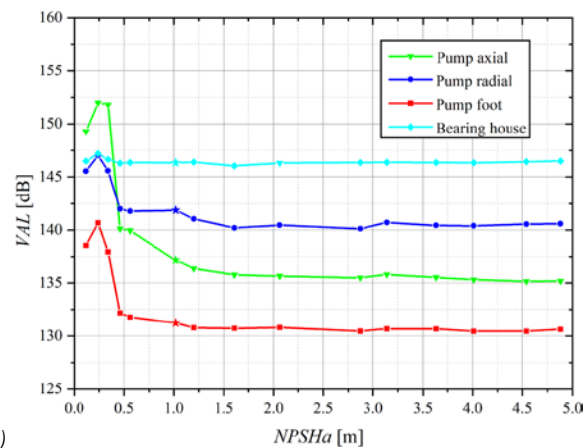
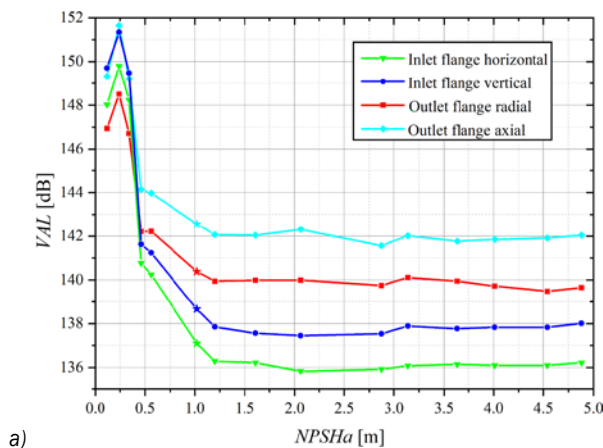


Fig. 8. Trends of the total VAL of each measuring point with NPSHa; a) inlet and outlet measuring points, and b) pump body measuring points.

At the same time, with the decrease of inlet pressure, the current affected by cavitation also changes obviously, and it has regularity. As shown in Fig. 7, during the process of NPSHa falling from 5 m to 2 m, the overall current shows a downward trend. When NPSHa = 2 m, the current decreases by 2 %, then there is a rebound. After the NPSHa drops below 1.2 m, the current decreases continuously. And when NPSHa is less than 0.5 m, the current drops sharply, by about 12 %. Therefore, consistent with the method proposed in [8], the onset of pump cavitation can be detected by the motor phase currents.

2.2 Structural Vibration Signals

The variation curves of vibration acceleration levels for each measuring point at different NPSHa as shown in Fig. 8. The vibration acceleration level at each measuring point fluctuates slightly during the non-cavitation stage but remains low. As the NPSHa reach the onset of cavitation, the vibration acceleration levels increase significantly, and as the degree of cavitation increases, the vibration acceleration levels rise rapidly after reaching the peak, and then decline. The results are close to the trend of the vibration acceleration on the pump casing in [10], and the rise rate of the vibration acceleration level at NPSHr is also similar.

Comparing the eight measuring points, the vibration acceleration level at the Bearing house is the highest. However, the overall curve change rate is relatively small, while the vibration acceleration levels of the other measuring points increase significantly during the cavitation development phase. The point marked by the star symbol in the figure is the head drop of 3 %, that is, the vibration acceleration level of each monitoring point at the NPSHr. The vibration acceleration level at the outlet flange is higher than that of the inlet flange. However, the amplitude change at the inlet flange is more pronounced, rising by approximately 0.6 % at NPSHr. In the non-cavitation stage, the vibration acceleration of the pump radially is larger than the pump axially. With the intensification of cavitation, the vibration acceleration level at the pump axial significantly exceeds that at the pump radial, and increases by about 0.5 % at NPSHr.

Fig. 9 shows the vibration acceleration levels spectrum with cavitation development at different measuring points. The trend of each measuring point shows that as the cavitation continues to increase, there is an evident broadband characteristic.

Continued over page >



FELIX

Everything in one place

Get more out of Asset Condition Monitoring.

Experience is retiring, and knowledge comes and goes more than ever. Everyone in your plant should have an interest in asset reliability, and Felix allows them to do so.

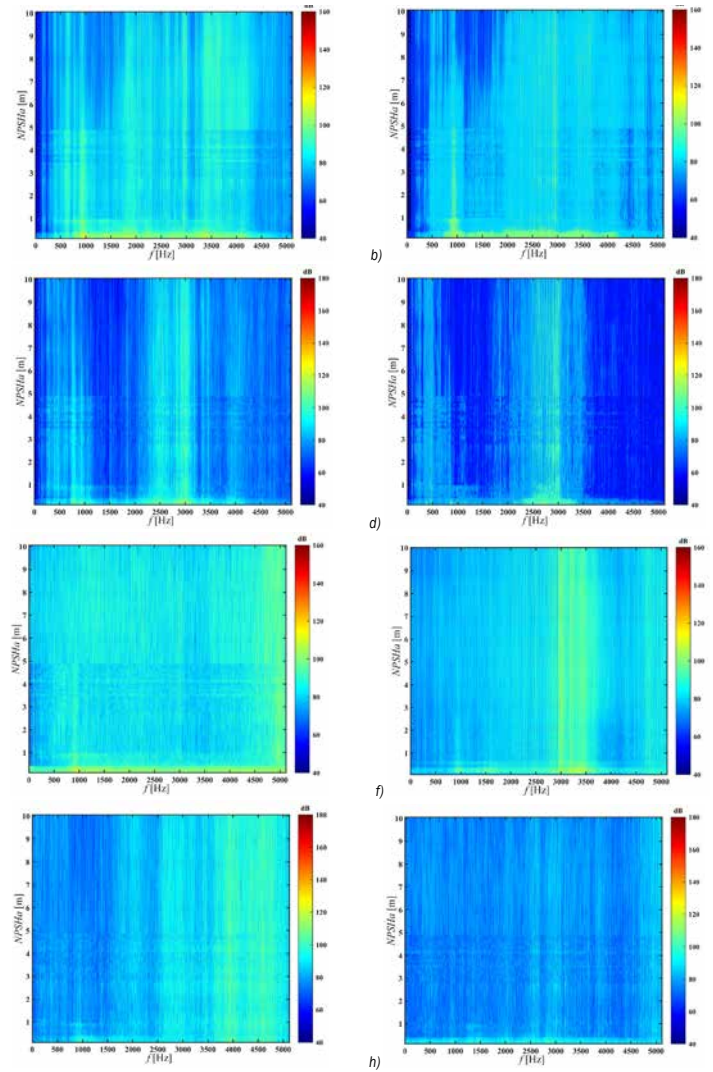
Felix is an enabler to turn your Condition Monitoring investment from a routine defect detection task to a defect elimination platform through a deeper understanding of what drives your failures.

www.felixhub.com

A simpler, smarter reporting system

Fig. 9. VAL frequency characteristics of each measuring point with NPSHa; a) inlet flange horizontal, b) inlet flange vertical, c) outlet flange radial, d) outlet flange axial, e) pump axial, f) pump radial, g) pump foot, and h) bearing house.

The inlet flange horizontal and vertical measuring points have a strong signal distribution in all frequency bands during the non-cavitation phase, but the overall distribution is dispersed. After the onset of cavitation, the vibration signal in the 500 Hz to 4500 Hz frequency band enhances significantly. The outlet flange measuring point is mainly concentrated below 1000 Hz and in the band of 2000 Hz to 3500 Hz. With the NPSHa decreasing, the signal change in the range of 2000 Hz to 3500 Hz is more obvious. In contrast, the inlet measuring point is more sensitive to the onset of cavitation. The pump body axial measuring point shows a strong vibration signal appears in all frequency bands. The spectrum distribution at the pump body radial is also broader, and the vibration acceleration level signal in 3000 Hz to 3500 Hz is intense. However, with the development of cavitation, the variation of the vibration acceleration level signal in the whole frequency range is not as pronounced as that of pump body axial. The bearing house measuring point has a relatively strong amplitude in the high-frequency band, while the overall vibration acceleration level of the pump foot is small, and the signal distribution is relatively sparse. Both spectral variations are not sufficiently apparent and less sensitive to the onset of cavitation.



2.3 Liquid-borne Noise Signals

With the decrease of inlet pressure, NPSHa continuously decreases, and the frequency domain of the peak signal of the inlet and outlet liquid-borne noise gradually shrinks, as shown in Fig. 10. As the cavitation effect intensifies, the signal above 120 dB inlet almost disappears. The sound pressure level in 1000 Hz to 5000 Hz at the outlet drops below 100 dB. The length of the vapour attached to the blade's working surface increases, and there are large oscillations in the tail of the cavitation.

It causes the bubbles to fall off, and the unstable cavitation intensifies, thus leading to broad frequency pulsations in the low-frequency band of the liquid-borne noise. Moreover, because the cavitation in part of the flow channel blocks the entry of the main flow, the number of effective flow channels is reduced, thereby changing the frequency distribution of the liquid-borne noise.

Continued over page >

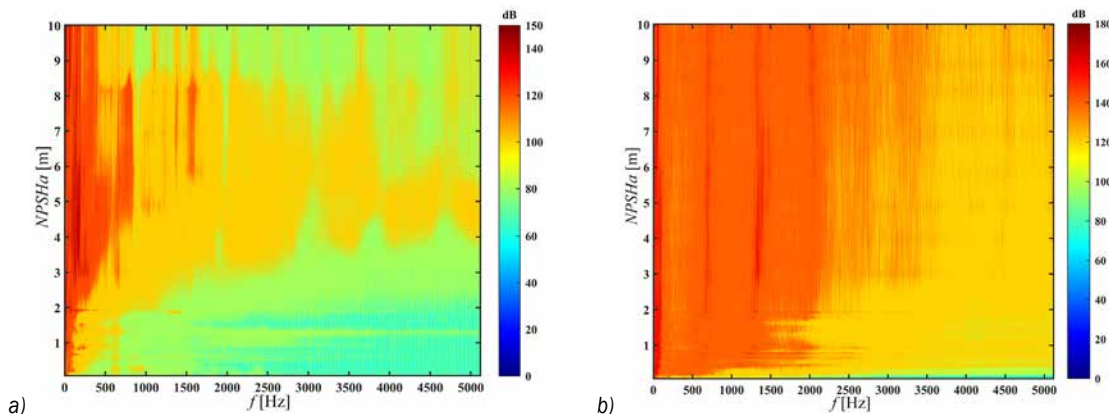


Fig. 10. Liquid-borne noise frequency characteristics; a) at the inlet, and b) at the outlet with NPSHa.

Monitor

The 8 Pillars of Ultrasound



Bearing Lubrication Monitoring:

Proper lubrication minimizes surface contact of machinery, and reduces undesired friction, excessive heat, metal-on-metal contact and wear and tear.



Hydraulic System Monitoring

Failure modes in hydraulics systems include external leakage, internal leakage, by-passing, and blockages.



Air & Gas leak Detection:

Undetected air & gas leaks are costly, inefficient, polluting, and sometimes unsafe.



Steam Trap Testing:

A fully-functional steam trap is energy-efficient and does not waste quality steam.



Mechanical Condition Monitoring:

Unexpected machine breakdowns threaten your bottom line, the environment, and worst of all, workers' safety.



Valve Condition Monitoring

Internal or external leaks, or issues with flow regulation in your valves threaten your factory.



Electrical Fault Detection:

Unreliable electric power system cost manufacturers millions in downtime and repairs and have the potential to maim and kill.



Underground Tank, Weather, & General Tightness Testing

When the tightness integrity of air tight compartments deteriorate, two things happen... Things leak out, and things get in.



Gain a better understanding of the health of your factory.



+61 (0) 2 49252701
sales@gvsensors.com.au

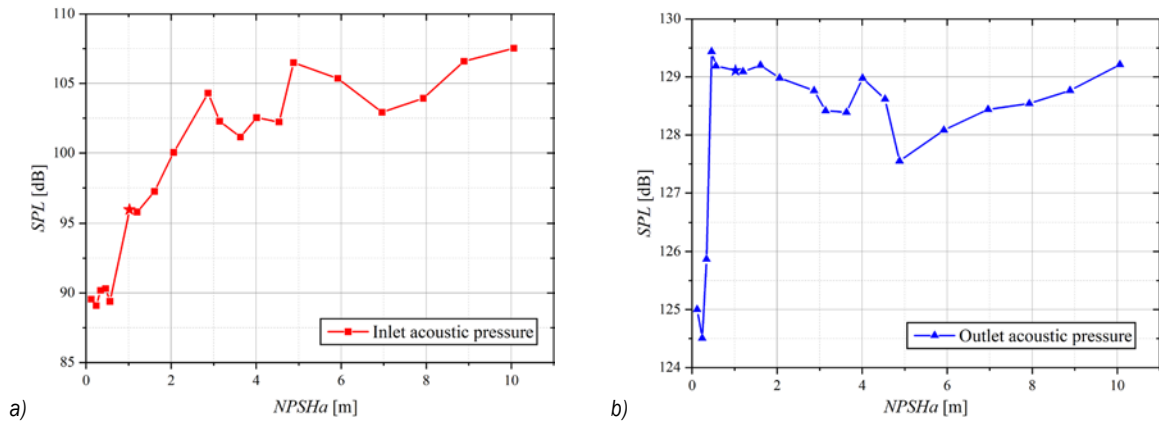


Fig. 11. Trends of a) inlet and b) outlet liquid-borne noise SPL with NPSHa.

Although there is also a more pronounced change in the outlet liquid-borne noise signal, the variation is insignificant compared to the inlet. Fig. 11 shows that with the decrease of the NPSHa, the inlet liquid-borne noise presents a continuous decreasing trend, which is similar to the trend in [10]. However, the sound pressure level of the liquid-borne noise at the outlet first decreased, then increased, and finally decreased rapidly. At the net positive suction head required point, the inlet liquid-borne noise decreases by approximately 14 %, while the outlet liquid-borne noise decreases by approximately 1 %. The comparison shows that the inlet liquid-borne noise measuring point is more sensitive to the outlet.

2.4 Pressure Pulsation Signals.

The power spectral density (PSD) method was used to process the pressure pulsation signal to determine the intensity of the pressure pulsation. Fig. 12 shows the pressure pulsation intensity coefficient as the NPSHa decreases. It can be found that the inlet pressure pulsation shows a decreasing trend with the reduction of the NPSHa, while the outlet pressure pulsation is maintained first and then rapidly rising trend. When the head drops by 3 %, the inlet pulsation intensity decreases by 66.3 %, while the outlet pulsation intensity increases by 13.9 %. The

inlet pulsation intensity shows an overall decreasing trend as the NPSHa decreases. Although there are some fluctuations, it can better reflect the pressure pulsation intensity change with the development of cavitation. The outlet pressure pulsation does not change significantly before the onset of cavitation. When it is close to complete cavitation, the sudden rise occurs, and the rate of change is not as apparent as the inlet measuring point. Therefore, relative to the measuring point at the outlet position, the pressure pulsation measuring point at the inlet can better predict the inception and development of cavitation.

3. Analysis of Numerical Simulation Results

3.1 Vapour Volume Evolution

Fig. 13 shows the evolution in the volume fraction distribution of vapour under different NPSHa. As the NPSHa decreases, the vapour volume in the impeller continues to extend from the blade inlet to the outlet. The development of vapor volume presented in the results is consistent with [4]. When the NPSHa is 1.61m, it is the inception of cavitation. A lower level of vapour has appeared on the suction surface of the blade inlet, but there is no significant change in head and flow rate. When the NPSHa is 1.34 m, the vapour volume area expands. At this time, the head does not

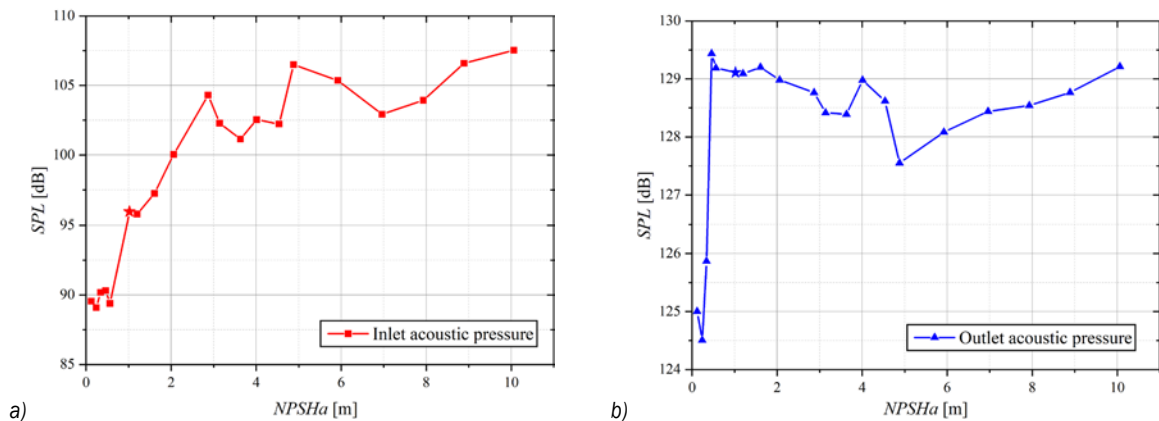


Fig. 12. Trends of a) inlet and b) outlet pressure pulsation PSD with NPSHa.

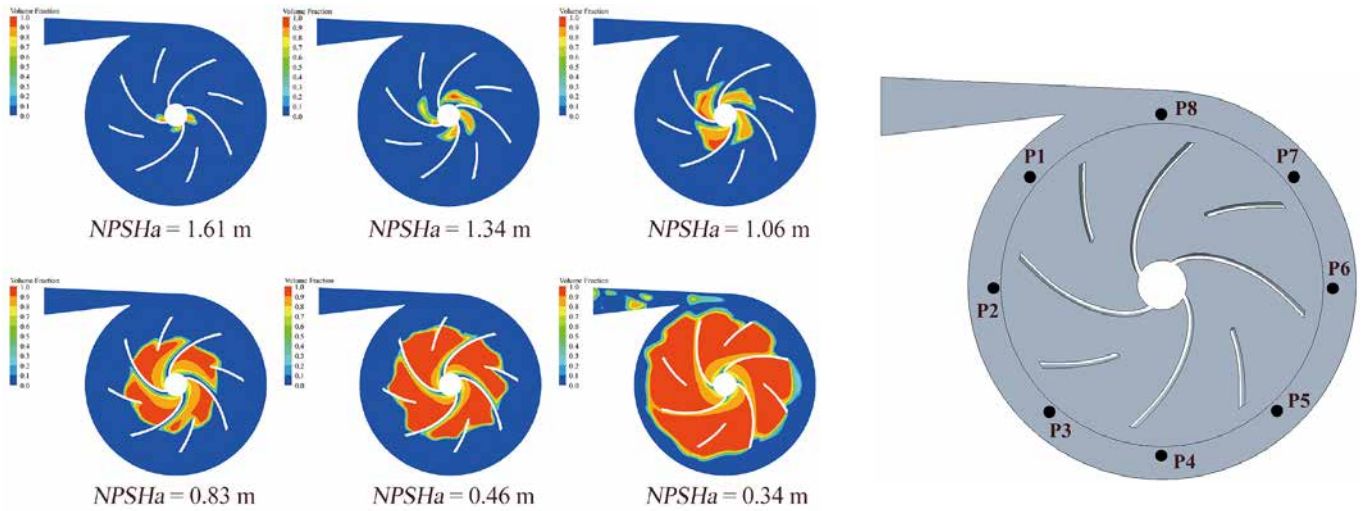


Fig. 13 (Above left). Volume fraction distribution of vapor under different NPSHa. **Fig. 14 (above right).** Pressure pulsation measuring points.

decrease but instead increases slightly, which is due to the bubbles generated on the blade surface, which improve the flow state in the pump. When approaching the NPSHr, the vapour area begins to diffuse towards the blade working surface, and the flow rate and head drop by approximately 2.8 % and 3 %, respectively. At NPSHa is 0.83, the vapour area spreads to the root of the splitter blade, occupying about one half of the flow channel, and the head drops by more than 5 %. While the flow rate drops slightly lags behind the head, dropping by about 3 %. As NPSHa continues to decline, the vapour area occupies the entire flow channel of the impeller and flows into the diffusion section of the volute, blocking the flow channel. The flow rate and head drop by 27 % and 13.4 %, the pump's performance is seriously affected.

3.2 Pressure Pulsation Analysis

To investigate the characteristic changes of the pressure pulsation signal in the pump under different NPSHa, eight pressure pulsation monitoring points were set up at the interface between the impeller and the volute, and each monitoring point is separated by 45°, as shown in Fig. 14. The stable results of the last three cycles are extracted from the unsteady calculation. The fast Fourier transform (FFT) algorithm was used to calculate the discrete Fourier transform (DFT) of the pressure pulsation time-domain signal at different cavitation stages at each measuring point. The frequency-domain results are shown in Fig. 15.

The impeller rotational speed is $n = 2900$ rpm, so the shaft frequency $f_r = 48.3$ Hz, the main blade passing frequency $f_{MBPF} = 193.3$ Hz, and the total blade passing frequency $f_{BPF} = 386.7$ Hz. In the non-cavitation phase, the main frequency of the pressure pulsation at the monitoring points P2 to P4 and P8 is the total blade passing frequency f_{BPF} of the impeller, which is eight times the shaft

frequency. The main frequency of P5 to P7 is the main blade passing frequency f_{MBPF} (i.e., four times the axis frequency). When cavitation causes a 3 % drop in head, the main frequency is at the main blade passing frequency f_{MBPF} at all six monitoring points except for P3 and P7, where the main frequency is at the f_{BPF} . When the head drops by 5 %, the main frequency at P1 appears at two times the shaft frequency. The main frequency P3 is at the main blade passing frequency f_{MBPF} . For other monitoring points, the main frequency is at the total blade passing frequency f_{BPF} . When the head drops sharply by 30 %, the main frequency of some monitoring points shift. Except for P4, P5, and P6 at the f_{BPF} , the main frequencies appear at the 1/3 and 2/3 shaft frequency. As cavitation develops and the amplitude of the pressure pulsation signal increases, the interference at harmonic frequencies becomes severe. The main frequency of some monitoring points also has some changes.

4. Conclusions

This paper studied the influence of measuring point distribution for pump cavitation diagnosis. The liquid-borne noise, vibration acceleration and pressure pulsation at different positions of the pump units were measured through the fixed valve test. The RMS was used to process the signal data of each cavitation condition, which can better reflect the sensitivity of monitoring points to cavitation than the data analysis at the characteristic frequency in [10] and [13]. The sensitivities of different measuring points to predict cavitation were compared. Furthermore, the SST k- ω turbulence model and Zwart cavitation model were used to numerically simulate the evolution of the vapour's volume distribution and pressure pulsation characteristics inside the pump.

Continued over page >

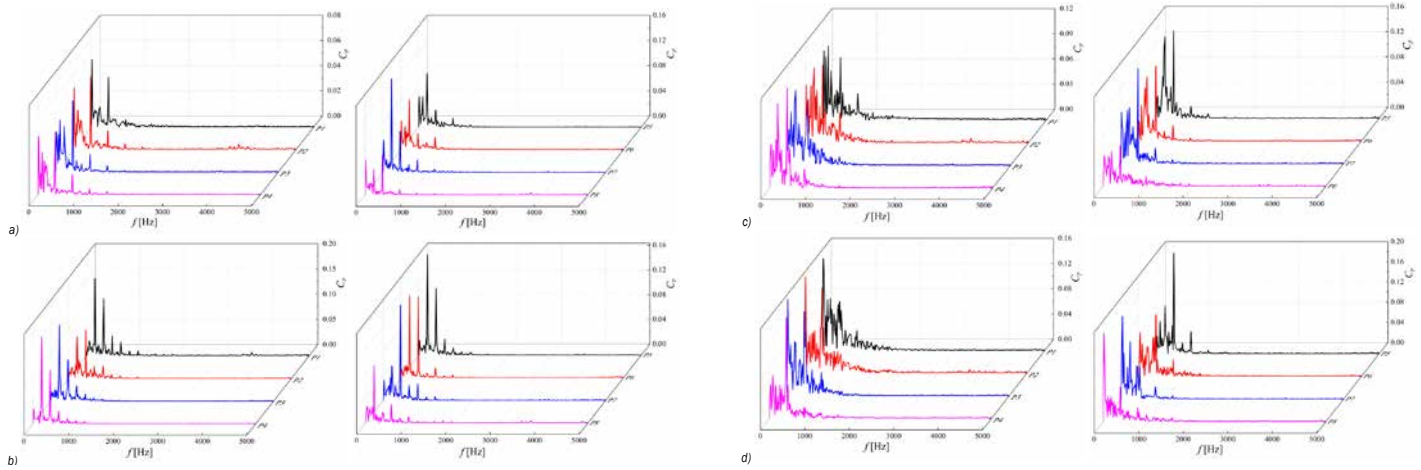


Fig. 15. Pressure pulsation frequency under different cavitation conditions; a) none-cavitation, b) 3 % drop in head, c) 5 % drop in head, d) 27 % drop in head.

With the development of cavitation, the flow rate decreases more slowly than the head. When the head drops by 3 %, the flow rate reduces by about 2.8 %. The motor current also shows a certain decrease, which can be used to predict the onset of cavitation and agrees with the findings [8]. When NPSHa is less than 0.5 m, the current drops sharply, about 12 %. The vibration acceleration level of each measuring point increases significantly. The measuring points of the inlet flange and the pump body axial are more sensitive to predicting cavitation, and both decreased by 0.6 %. The frequency band of the liquid-borne noise peak shrinks significantly. At the NPSHr operating point, the sound pressure level of the inlet liquid-borne noise decreases by 14 %, while the outlet decreases by 1 %, so the inlet liquid-borne noise measuring point is better for cavitation prediction. The inlet pressure pulsation intensity shows a decreasing trend, while the outlet is the opposite. The rate of change of inlet pressure pulsation intensity is more pronounced than the outlet. When the head drops by 3 %, the inlet pulsation intensity decreases by 66.3 %, while the outlet pulsation intensity increases by 13.9 %. The main frequency of the pressure pulsation signal is mainly distributed at the total blade passing frequency f_{BPF} . However, with the development of cavitation, the main frequency is influenced by the harmonic frequency, and some of the main frequencies are shifted. In summary, the inlet flange and pump casing axial vibration measuring points, inlet liquid-borne noise, and pressure pulsation measuring points have superior sensitivity and are suitable for cavitation fault diagnosis.

The arrangement of measuring points for cavitation fault diagnosis proposed in this work can be effectively applied to other pumps. The proposed method can be extended to the diagnosis of other pump faults, such as impeller damage, shaft misalignment, and shaft imbalance. However, regarding the thresholds for

fault signal prediction, since different types of pumps have different performances and requirements, it is necessary to make specific judgments according to the actual situation. It can be further investigated in subsequent studies to improve the accuracy of cavitation fault diagnosis.

5. Acknowledgements

The authors would like to thank the financial support from National Natural Science Foundation of China (No. 51879122, 51779106), National Key Research and Development Program of China (Grant No. 2016YFB0200901, 2017YFC0804107), Zhenjiang key research and development plan (GY2017001, GY2018025), the Open Research Subject of Key Laboratory of Fluid and Power Machinery, Ministry of Education, Xi-hua University (szjj2017094, szjj2016068), Sichuan Provincial Key Lab of Process Equipment and Control (GK201614, GK201816), Jiangsu University Young Talent training Program-Outstanding Young backbone Teacher, Program Development of Jiangsu Higher Education Institutions (PAPD), and Jiangsu top six talent summit project (GDZB-017).

6. References

- [1] Guan, X.F. (1995). Handbook of Modern Pump Technology, Astronautic Press, China.
- [2] Guo, X., Zhu, L., Zhu, Z., Cui, B., Li, Y. (2015). Numerical and experimental investigations on the cavitation characteristics of a high-speed centrifugal pump with a splitter-blade inducer. Journal of Mechanical Science and Technology, vol. 29, p. 259-267, DOI:10.1007/s12206-014-1232-x.
- [3] Luo, X.W., Ji, B., Tsujimoto, Y. (2016). A review of cavitation in hydraulic machinery. Journal of Hydrodynamics, vol. 28, p. 335-358, DOI:10.1016/S1001-6058(16)60638-8.
- [4] Dong, L., Shang, H., Zhao, Y., Liu, H., Wang, Y. (2019). Study on unstable characteristics of centrifugal pump under different cavitation stages. Journal of Thermal Science, vol. 28, p. 608-620, DOI:10.1007/s11630-019-1136-2.
- [5] Al-Obaidi, A.R. (2019). Effects of different turbulence models on three-dimensional unsteady cavitating flows in the centrifugal pump and performance prediction. International Journal of Nonlinear Sciences and Numerical Simulation, vol. 20, no. 3-4, p. 487-509, DOI:10.1515/ijnsns-2018-0336.
- [6] ISO 3555 (1977). Centrifugal, Mixed Flow and Axial Pumps-Code for Acceptance Tests-Class B. International Organization for Standardization, Geneva.
- [7] Stopa, M.M., Cardoso Filho, B.J., Martinez, C.B. (2013). Incipient detection of cavitation phenomenon in centrifugal pumps. IEEE Transactions on Industry Applications, vol. 50, no. 1, p. 120-126, DOI:10.1109/TIA.2013.2267709.
- [8] Harihara, P.P., Parlos, A.G. (2006). Sensorless detection of cavitation in centrifugal pumps. ASME International Mechanical

Mobius Institute wants to help you

ACHIEVE YOUR GOALS™

Mobius Institute™ helps condition monitoring, maintenance, and asset reliability practitioners, business leaders, and strategic partners achieve the next level of success through leading-edge training, accredited certification, engaging conferences, and educational websites.



Professional Growth

Move to the Next Level in Your Career

Gain the education and internationally recognized certification to take your career to the next level



Corporate Reliability

Improve Reliability and Performance

Educate your team or follow our Asset Reliability Transformation® [ART] process to improve your site's performance



START HERE!
mobiusinstitute.com



WORD BUILDER

How many words of three or more letters can you make, using each letter only once? Plurals are allowed, but no foreign words or words beginning with a capital. There is at least one 5 letter word.

15 - Good | 20 - Very Good | 30+ - Excellent

R	H	A	E	S
---	---	---	---	---

There is 5 possible 5 letter words above. Can you find them all?

WORD MARCH

Draw a path from one square to another to find the secret nine letter word. You may move in any direction. Each square can only be used once.

There are approx. 220 words (four letters or more) that can be made from the combination of letters below. How many can you make?

Solution on page 38.

A	R	T
T	S	E
A	G	M

Nine letter word is... _____

SODUKU

To solve, each number from 1 to 9 must appear once in:

- Each of the nine vertical columns
- Each of the nine horizontal rows
- Each of the nine 3 x 3 boxes

No number can be repeated twice in a box, row or column. Why not time yourself? **We've started it off for you...**

9			3	4			1	
	5				6			
4	7					5	6	
6								
	3	4	1				8	
			5		8			7
5	6				3			
			6	8		1		
1		7	2	5	4			

Engineering Congress and Exposition, p. 187-192, DOI:10.1115/IMECE2006-14655.

[9] Al-Hashmi, S., Gu, F., Li, Y., Ball, A. D., Fen, T., Lui, K. (2004). Cavitation detection of a centrifugal pump using instantaneous angular speed. *Engineering Systems Design and Analysis*, p. 185-190, DOI:10.1115/ESDA2004-58255.

[10] Čudina, M., Prezelj, J. (2009). Detection of cavitation in situ operation of kinetic pumps: effect of cavitation on the characteristic discrete frequency component. *Applied Acoustics*, vol. 70, no. 9, p. 1175-1182, DOI:10.1016/j.apacoust.2009.04.001.

[11] Čudina, M. (2003). Noise as an indicator of cavitation in a centrifugal pump. *Acoustical Physics*, vol. 49, no. 4, p. 463-474, DOI:10.1134/1.1591303.

[12] Čudina, M. (2003). Detection of cavitation phenomenon in a centrifugal pump using audible sound. *Mechanical Systems and Signal Processing*, vol. 17, no. 6, p. 1335-1347, DOI:10.1006/mssp.2002.1514.

[13] Černetič, J. (2009). The use of noise and vibration signals for detecting cavitation in kinetic pumps. *Proceedings of the Institution of Mechanical Engineers, Part C: Journal of Mechanical Engineering Science*, vol. 223, no. 7, p. 1645-1655, DOI:10.1243/09544062JMES1404.

[14] Černetič, J., Čudina, M. (2011). Estimating uncertainty of measurements for cavitation detection in a centrifugal pump. *Measurement*, vol. 44, no. 7, p. 1293-1299, DOI:10.1016/j.measurement.2011.03.023.

[15] Chini, S.F., Rahimzadeh, H., Bahrami, M. (2005). Cavitation detection of a centrifugal pump using noise spectrum. *International Design Engineering Technical Conferences and Computers and Information in Engineering Conference*, p. 13-19, DOI:10.1115/DETC2005-84363.

[16] Wang, Y., Liu, H., Yuan, S., Tan, M., Wang, K. (2012). Experimental testing on cavitation vibration and noise of centrifugal pumps under off-design conditions. *Transactions of the Chinese Society of Agricultural Engineering*, vol. 28, no. 2, p. 35-38, DOI:10.3969/j.issn.1002-6819.2012.02.007. (in Chinese)

[17] Zhang, N., Yang, M., Gao, B., Li, Z. (2015). Vibration characteristics induced by cavitation in a centrifugal pump with slope volute. *Shock and Vibration*, vol. 2015, art. ID 294980, DOI:10.1155/2015/294980.

[18] Dong, L., Zhao, Y., Dai, C. (2019). Detection of inception cavitation in centrifugal pump by fluid-borne noise diagnostic. *Shock and Vibration*, vol. 2019, art. ID 9641478, DOI:10.1155/2019/9641478.

[19] Al-Obaidi, A. R. (2020). Experimental comparative investigations to evaluate cavitation conditions within a centrifugal pump based on vibration and acoustic analyses techniques. *Archives of Acoustics*, vol. 45, no. 3, p. 541-556, DOI:10.24425/aoa.2020.134070.

[20] Al-Obaidi, A. R. (2019). Investigation of effect of pump rotational speed on performance and detection of cavitation within a centrifugal pump using vibration analysis. *Heliyon*, vol. 5, no. 6, art. ID e01910, DOI:10.1016/j.heliyon.2019.e01910.

[21] Al-Obaidi, A.R. (2020). Detection of cavitation phenomenon within a centrifugal pump based on vibration analysis technique in both time and frequency domains. *Experimental Techniques*, vol. 44, p. 329-347, DOI:10.1007/s40799-020-00362-z.

[22] Al-Obaidi, A.R., Mishra, R. (2020). Experimental investigation of the effect of air injection on performance and detection of cavitation in the centrifugal pump based on vibration technique. *Arabian Journal for Science and Engineering*, vol. 45, p. 5657-5671, DOI:10.1007/s13369-020-04509-3.

[23] Mousmoulis, G., Karlsen-Davies, N., Aggidis, G., Anagnostopoulos, I., Papantonis, D. (2019). Experimental analysis of cavitation in a centrifugal pump using acoustic emission, vibration measurements and flow visualization. *European Journal of Mechanics-B/Fluids*, vol. 75, p. 300-311, DOI:10.1016/j.euromechflu.2018.10.015.

[24] Pan, Z.Y., Yuan, S.Q. (2013). *Fundamentals of Cavitation in Pumps*, Jiangsu University Press, Jiangsu.

[25] Dong, L., Zhao, Y.Q., Dai, C., Wang, Y. (2018). Research on cavitation acoustic characteristics of centrifugal pump based on fluid-acoustic field coupling method. *Advances in Mechanical Engineering*, vol. 10, no. 5, DOI:10.1177/1687814018773665.

[26] Yu, H. (2016). *Vibration Noise Measurement and Analysis Technology of Ship*. China Light Industry Press, p. 4-11.

[27] Du, G. (2012). *Acoustic Fundamentals*. Nanjing university Press, Nanjing, p. 127-128.

[28] Alahmadi, Y., Nowakowski, A. (2016). Modified shear stress transport model with curvature correction for the prediction of swirling flow in a cyclone separator. *Chemical Engineering Science*, vol. 147, p. 150-165, DOI:10.1016/j.ces.2016.03.023.

TEST YOUR KNOWLEDGE - PART 68 OF A SERIES

1 An electric motor fitted with a 300 mm diameter pulley runs at 1500 rpm. The belt length is 3500 mm. What is the belt-passing frequency (approximately)?

- a 3.7 Hz
- b 6.7 Hz
- c 8.7 Hz
- d 12.7 Hz

2 As a general rule, what is the range either side of running speed that should be free of natural frequencies to avoid running in resonance?

- a +/- 2%
- b +/- 5%
- c +/- 10%
- d +/- 20%

3 The P-F Curve is an important component of RCM. Which era do you think it was first developed?

- a 1950s
- b 1960s
- c 1970s
- d 1080s

4 A 4-pole motor is driven by a VSD at a speed of 1200 rpm. If the motor were to display vibration at 2 x electrical line frequency, what would be the approximate frequency of that vibration?

- a 40 Hz
- b 50 Hz
- c 80 Hz
- d 100 Hz

5 Some hardware and software packages allow the user to view their spectra with a logarithmic amplitude scale. Where might you find this useful?

- a If you wish to see lower amplitude data amongst higher amplitude data
- b If you are wanting to examine the phase of the signals
- c If you want to improve the frequency resolution of the data
- d Both A and B

6 For a belt-driven fan installation, which of the following mounting systems is likely to offer the best isolation at low frequencies?

- a Rubber mat.
- b Rubber-based resilient mount
- c Spring mounting system
- d Hard-bolted interface between fan frame and concrete

7 Which of the following might be considered when investigating the onset of cavitation in a pumping system?

- a NPSH
- b GST
- c VAT
- d APEC

8 Which of the following settings is likely (over time) to influence the size of your vibration database?

- a The lines of resolution for spectral data
- b The amplitude of the vibrations being measured
- c The maximum frequency of the spectral data
- d Both A and B

9 You have been asked to “gap” some prox probes for a steam turbine. In the absence of any other information, which of the following gap voltages would you aim for?

- a -1 volt
- b -2 volt
- c -10 volt
- d -100 volt

10 The 2022 VANZ conference will be held in which location?

- a Whangarei
- b Hamilton
- c Queenstown
- d Wairakei



Answers on page 38

Spectrum



The official journal of the Vibrations Association of New Zealand (VANZ)

Our quarterly magazine includes:

- Papers from conference reprinted
- Conference information
- Articles and reports from industry leaders
- Presidents report
- Notices
- Committee reports
- Interactive activities *and much more..*



Advertising Rates

DPS	Full Page	Half Page	Quarter Page	Advertorial
Size (width x height): 420x297mm (Trim) 426x303mm (Bleed)	Size (width x height): 210x297mm (Trim) 216x303mm (Bleed)	Size (width x height): 190x134mm (Horz) 93x272mm (Vert)	Size (width x height): 190x80mm (Horz) 93x134mm (Vert)	\$100 per page or 50% discount if bought in conjunction with a full page colour advert.
Single issue rate: \$550+GST	Single issue rate: \$350+GST	Single issue rate: \$300+GST	Single issue rate: \$250+GST	
4-issue (1 year) rate: \$500+GST	4-issue (1 year) rate: \$315+GST	4-issue (1 year) rate: \$270+GST	4-issue (1 year) rate: \$225+GST	

The small print...

How to supply an advert:

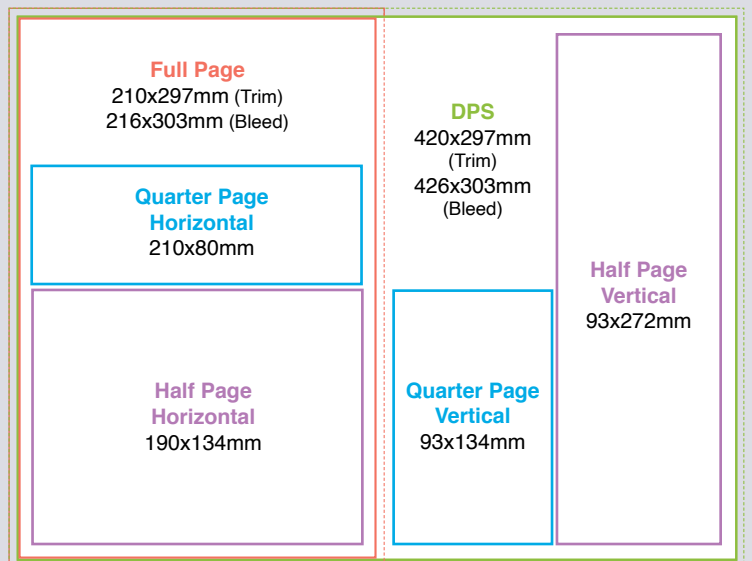
All advertising copy to be supplied in high-res PDF format at the correct size required. Files to be supplied press ready at 300dpi with 3mm bleed for full page and DPS advertisements. The special 4-issue rates are for advertising in 4 consecutive issues. i.e. Issue 91, 92, 93 and 94. **Save up to \$200 on your advertising in Spectrum!** Email Angie at spectrumeditor@vanz.org.nz to confirm your advert(s) and method of payment as soon as possible.

Publishing:

Each SPECTRUM will be distributed as an epub document and available for download and printing by VANZ members. Previous issues will become available on the public domain.

Article submissions:

Articles for upcoming issues of Spectrum are welcomed by the editor. Copy to be supplied preferably in Microsoft Word, but PDF file format is also acceptable. Please email spectrumeditor@vanz.org.nz with your submission or should you require further information.



Word March: stratagem | Word Builder: share, hares, shares, shear, hears, hears, hears
1B, 2D, 3C, 4C, 5A, 6C, 7A, 8A, 9C, 10D
Answers to Carlton Technology Quiz 68:



Brüel & Kjær Vibro

A member of the NSK Group

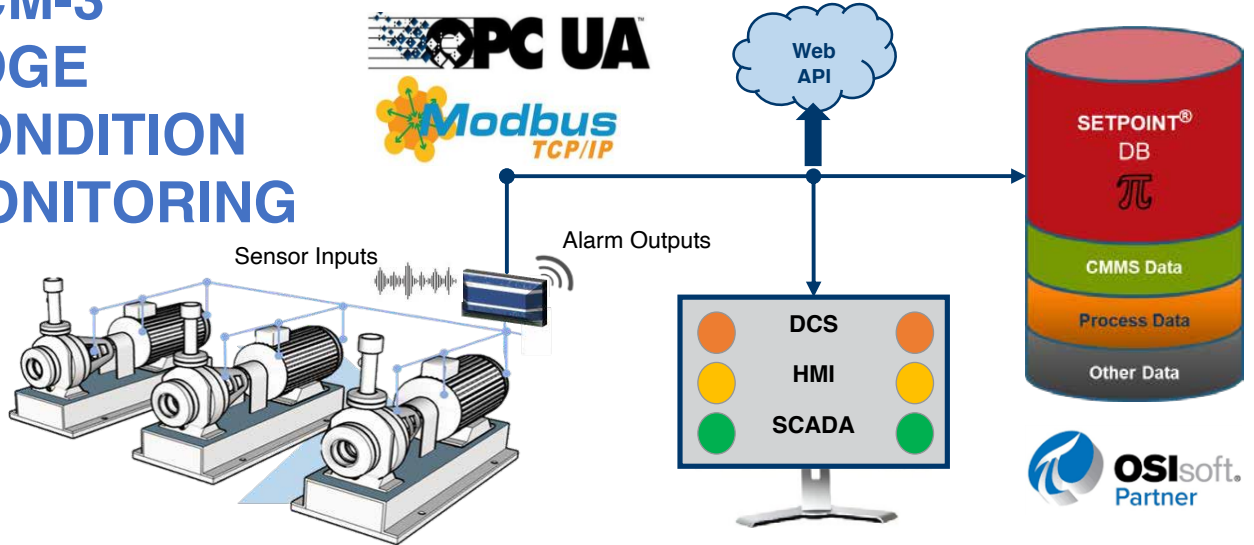
ASSET HEALTH MONITORING FOR OPERATIONS AND MAINTENANCE



VCM-3 – Project Machine Health to Maximize Uptime



VCM-3 EDGE CONDITION MONITORING



For more information, please refer to BKVibro Website:

<https://www.bkvibro.com/product/vcm-3/>

Enquire Now: sales@cse-waf.nz

The next step in your digital transformation just got easier!



Emerson's AMS Wireless Vibration Monitor is based on decades-proven technology that communicates using modern, cybersecure protocols. This is the wireless device that will extend your reliability program to an unprecedented number of plant assets – including those in hazardous or hard to reach areas – and deliver maximum visibility to asset health.

The unit features complete data acquisition – triax vibration with temperature and PeakVue measurements – to provide a sophisticated look at asset health on par with other online and portable monitoring options.

Ideal for deployment across your plant or enterprise, the AMS Wireless Vibration Monitor offers the following benefits:

- Automated machine monitoring with a lower total cost of ownership.
- Simple installation in about 5 minutes.
- Fleet management tools for fast configuration in the shop or in the field.
- Prescriptive analytics using patented PeakVue Plus to accelerate your diagnosis.

- Reduced time in the field – more time to recommend maintenance actions.
- Rapid ROI with lower installed cost and fast access to actionable information.
- Long 3-5 year life with an off-the-shelf battery collecting up to 4 waveforms per day.
- Battery replacement in the field – even in hazardous areas.
- Access asset health information on your mobile phone anytime, anywhere.

For More Information

The AMS Wireless Vibration Monitor is an integral part of the Emerson portfolio of portable and online machinery monitoring technology. Make it an integral part of your digital transformation journey today.

Visit our website at

www.emerson.com/AMSVibrationMonitor, or contact your local Emerson representative.



AMS